AFML-TR-71-188

MATERIALS PROCESSING OF RARE EARTH COBALT PERMANENT MAGNETS

P. J. JORGENSEN
R. W. BARTLETT
Stanford Research Institute

TECHNICAL REPORT AFML-TR-71-188

August 1971

AIR FORCE MATERIALS LABORATORY
AIR FORCE SYSTEMS COMMAND
WRIGHT-PATTERSON AIR FORCE BASE, OHIO 45433

Unclassified

Security Classification

DOCUMENT CONTROL DATA - R & D

Security classification of title, body of abstract and indexing annotation must be entered when the overall report is classified)

1 ORIGINATING ACTIVITY (Corporate author)

Stanford Research Institute
333 Ravenswood Avenue
Menlo Park, California 94025

2a. REPORT SECURITY CLASSIFICATION
Unclassifed

2b. GROUP

3 REPORT TITLE

MATERIALS PROCESSING OF RARE EARTH COBALT PERMANENT MAGNETS

4 DESCRIPTIVE NOTES (Type of report and inclusive dates)
Second Semi-Annual Interim Technical Report; January 1 to June 30, 1971

5 AUTHOR(S) (First name, middle initial, last name)

Paul J. Jorgensen
Robert W. Bartlett

6 REPORT DATE	7a. TOTAL NO. OF PAGES	7b. NO OF REFS
August 1971	65	5

8a. CONTRACT OR GRANT NO	9a. ORIGINATOR'S REPORT NUMBER(S)
F33615-70-C-1624	PYU-8731
b. PROJECT NO. ARPA Order No. 1617	
c. Program Code No. OD10	9b. OTHER REPORT NO(S) (Any other numbers that may be assigned this report) AFML-TR-71-188
d.	

10 DISTRIBUTION STATEMENT

Approved for public release; distribution unlimited.

11 SUPPLEMENTARY NOTES	12. SPONSORING MILITARY ACTIVITY
	Air Force Materials Laboratory Wright Patterson Air Force Base Ohio 45433

13 ABSTRACT

Rare earth-cobalt intermetallic compounds show promise for permanent magnets with a higher energy product, $(BH)_{max}$, than are currently available. Because fine particles are required for magnetic alignment and sintering, and since the coercivities of these fine particles are sensitive to overgrinding and particle surface preparation, various powder preparation techniques are being investigated as alternative methods for producing strain-free particles.

Methods that have been investigated include plasma spheroidization, plasma annealing, electrodeposition in fused salts, electrodeposition in organic liquids, direct reduction from amalgam droplets, precipitation from liquid zinc alloy solutions and direct metallothermic reduction.

Electrolysis in organic liquids and direct reduction from amalgam droplets yielded powders that were poorly crystallized with very inferior magnetic properties. The particles produced by precipitation from liquid zinc alloy solutions sintered during the precipitation process and since the precipitation occurred at temperatures above the Curie temperatures the particles were randomly oriented and therefore required grinding. This process thus did not provide any distinct advantages over conventional processing techniques. Plasma spheroidization and plasma annealing currently yields particles having reduced coercivities. This, however, does not exclude these powders as starting materials for powder metallurgical processing of rare earth-cobalt magnets, since a complete evaluation of these processes requires sintering of the powders followed by magnetic measurements.

DD FORM 1 NOV 68 1473 (PAGE 1)

S/N 0101-807-6801

Security Classification

14 KEY WORDS	LINK A		LINK B		LINK C	
	ROLE	WT	ROLE	WT	ROLE	WT
Magnetic Particles						
Rare Earth						
Cobalt						
Plasma Spheroidization						
Electrodeposition						

MATERIALS PROCESSING OF RARE EARTH COBALT PERMANENT MAGNETS

P. J. JORGENSEN
R. W. BARTLETT

FOREWORD

This is the second semiannual interim technical report of the research program "Materials Processing of Rare Earth-Cobalt Permanent Magnets" under Contract F33615-70-C-1624. Stanford Research Institute project number is PYU-8731. This project is being conducted by the Materials Laboratory of Stanford Research Institute. Dr. Paul J. Jorgensen, Manager of the Ceramics Group, is the project supervisor. Dr. Robert W. Bartlett of Stanford University is project consultant. Dr. M. Nisenoff made the magnetic measurements. The research described in this report is part of the contractual research program of the Materials Physics Division, Air Force Materials Laboratory, Air Force Systems Command, Wright-Patterson AFB, Ohio. It was sponsored by the Advanced Research Projects Agency, ARPA Order No. 1617, Program Code No. OD10.

This report covers research conducted between January 1, 1971 and June 30, 1971.

This technical report has been reviewed and is approved.

Charles E. Ehrenfried

CHARLES E. EHRENFRIED
Major, USAF
Chief, Electromagnetic Materials Branch
Materials Physics Division
Air Force Materials Laboratory

ABSTRACT

Rare earth-cobalt intermetallic compounds show promise for permanent magnets with a higher energy product, BH_{max}, than are currently available. Because fine particles are required for magnetic alignment and sintering, and since the coercivities of these fine particles are sensitive to over-grinding and particle surface preparation, various powder preparation techniques are being investigated as alternative methods for producing strain-free particles.

Methods that have been investigated include plasma spheroidization, plasma annealing, electrodeposition in fused salts, electrodeposition in organic liquids, direct reduction from amalgam droplets, precipitation from liquid zinc alloy solutions and direct metallothermic reduction.

Electrolysis in organic liquids and direct reduction from amalgam droplets yielded powders that were poorly crystallized with very inferior magnetic properties. The particles produced by precipitation from liquid zinc alloy solutions sintered during the precipitation process and since the precipitation occurred at temperatures above the Curie temperatures the particles were randomly oriented and therefore required grinding. This process thus did not provide any distinct advantages over conventional processing techniques.

Plasma spheroidization and plasma annealing currently yields particles having reduced coercivities. This, however, does not exclude these powders as starting materials for powder metallurgical processing of rare earth-cobalt magnets, since a complete evaluation of these processes requires sintering of the powders followed by magnetic measurements.

CONTENTS

ILLUSTRATIONS

LIST OF TABLES

I INTRODUCTION

The rare earth-cobalt intermetallic compounds having the composition $RECo_5$ exhibit high magnetic saturation and very high magnetocrystalline anisotropy. Permanent magnets can be made by magnetic alignment of fine particles and sintering. However, the coercive force of these materials initially increases as grinding proceeds and then passes through a maximum. The reasons for the decrease in coercive force with increased particle comminution is not well understood but has been attributed to imperfections caused by the grinding process. Significant increases in the coercive force have been achieved by etching the ground particles to remove surface material.

The objective of the present program is to investigate materials processing techniques that do not require grinding as the last step in producing powders suitable for either sintering or bonding with organic adhesives. The techniques developed are expected to reduce particle imperfections and strains which may yield higher coercivities.

Two general techniques for the production of fine $RECo_5$ particles are being emphasized: (1) spheroidization of previously comminuted particles dispersed in an inert gas plasma, and (2) electrodeposition or other solution deposition of $RECo_5$ particles at temperatures below the $RECo_5$ peritectic. The program has been divided into two tasks for the two materials processing techniques, and a third task for materials evaluation.

The primary material of this study is $SmCo_5$, but to provide greater insight into the general potential of each process studied, $PrCo_5$ has also been processed and evaluated.

II PLASMA SPHEROIDIZATION

A. Introduction

An inert gas arc plasma is being used to melt and spheroidize rare earth-cobalt alloy particles. More recently, $SmCo_5$ particles have been subjected to samarium vapor getter-annealing and hot chlorine etching in the arc plasma. The arc plasma apparatus has been previously described.[1] It provides for dispersion and injection of the particles normal to the plasma flow. Argon passed over hot calcium chips is used for the plasma gas and to convey particles into the plasma chamber. The sensible heat that the particles acquire can be controlled within a limited range by varying the power level and point of particle injection.

The plasma feed materials are cold hearth arc-melted alloys ball milled in hexane. The grinding details and precautions to prevent contamination have been previously described.[1] Annealing to achieve a homogeneous composition is required prior to grinding for the RE_2Co_7 alloys that were used for feed materials in some of the experiments.

Most of the particles attach to the chamber walls after passing through the plasma, and therefore the plasma chamber is rigged as a vacuum glove box so that these particles can be dislodged into a container attached to the plasma chamber with a vacuum port. After each plasma run the particles can be removed and transported to a glove box without air contamination.

Plasma melting and spheroidization have been investigated for cobalt alloys of samarium and praseodymium. A minor amount of work has been done on mischmetal alloys. Alloys with the $RECo_5$ and RE_2Co_7 compositions have

---

[1] AFML-TR-71-30, First Semiannual Technical Report.

been used. A major problem associated with these experiments is the vapor loss of rare earths on melting causing a shift in particle composition and, following solidification, particles with a two-phase microstructure.

Plasma heat treating permits a study of the effect of high temperature reduction and other high temperature reactions on the magnetic properties of individual particles without encountering sintering, which would occur in conventional furnace operations.

Plasma getter-annealing has been employed on $SmCo_5$ particles. A minor amount of samarium-rich low-melting particles is also included with the feed. Much of this samarium vaporized in the plasma and should limit the oxidation of the primary magnetic $SmCo_5$ particles, which are not melted.

Simultaneous annealing and etching of $SmCo_5$ particles without melting has been accomplished by adding small amounts of chlorine to the particle feed gas stream. Volatile chlorides of both samarium and cobalt were produced and condensed downstream.

B. Alloy Plasma Melting and Spheroidization

A large number of plasma spheroidization runs were made using $SmCo_5$ and $PrCo_5$ particles smaller than about 10 microns at various operating conditions to achieve melting while minimizing excess heating and rare earth vaporization losses. The plasma-spheroidized particles were examined by microscopy, x-ray diffraction, and electron beam microprobe analysis of individual particles. The results show that it is not possible to melt all the $SmCo_5$, or $PrCo_5$, particles passing through the plasma without losing substantial amounts of samarium, or praseodymium, and thereby causing precipitation of RE_2Co_{17} as well as $RECo_5$ phases within the quenched spherical particles. The Sm-Co phase diagram is shown in Figure 1; the Pr-Co phase diagram is similar.

Although praseodymium has a much lower vapor pressure than samarium, vaporization losses from liquid particles and other processing characteristics for praseodymium-cobalt alloys are about the same as for the

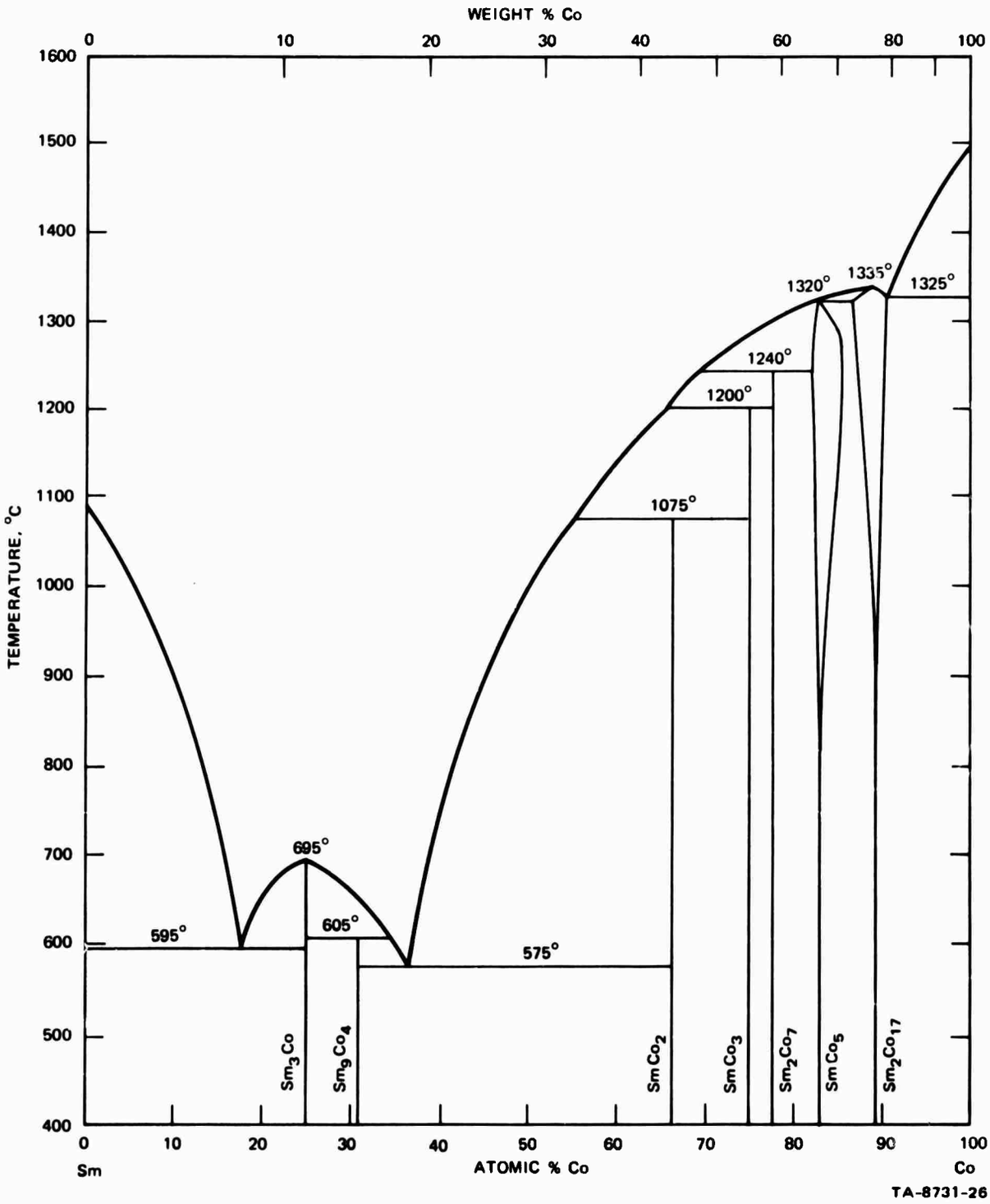

FIGURE 1 SAMARIUM-COBALT PHASE DIAGRAM

corresponding samarium alloys. This suggests that the slow process step controlling the rate of vaporization in these very small droplets with a high surface area to volume ratio may be diffusion of the rare earth element within the liquid droplet to the droplet surface, rather than the vaporization step itself. No measurable loss of samarium or praseodymium occurs during plasma heating of a particle unless the particle melts. Since the equilibrium vapor pressure of solid and liquid at the melting point must be identical if they have the same composition, this supports the diffusion limited hypothesis for vaporization. Typical liquid metal diffusion coefficients are in the range from 10^{-4} to 10^{-6} cm^2/sec whereas diffusion coefficients in solid alloys are usually several orders of magnitude smaller, even at temperatures just below their melting point. With either rare earth alloy, a submicron fume, containing higher concentrations of samarium or praseodymium than contained in the starting alloys, is produced by condensation of the vapor and some of the fume is collected concurrently with the major spheroidized particles. A scanning electron micrograph of spherical particles with adherent fume is shown in Figure 2. The composition of the fume indicates that some cobalt is also vaporized.

Because of the rapid quench of the droplets leaving the plasma, crystalline perfection of the spherical particles and the resulting x-ray diffraction patterns were poor. Metallographic examinations indicate that the grain size within these two-phase spherical particles is extremely small, about one micron (see Figure 3). The grains within a spherical particle tend to be randomly oriented, and magnetic alignment of such particles does not yield high magnetization.

Additional spheroidization runs were made using ground Sm_2Co_7 and Pr_2Co_7 particles so that the higher rare earth concentration in the starting material would compensate for vaporization losses in the plasma. The composition of particles is shifted, and one pass through the plasma yields an average composition midway between that of RE_2Co_7 and $RECo_5$.

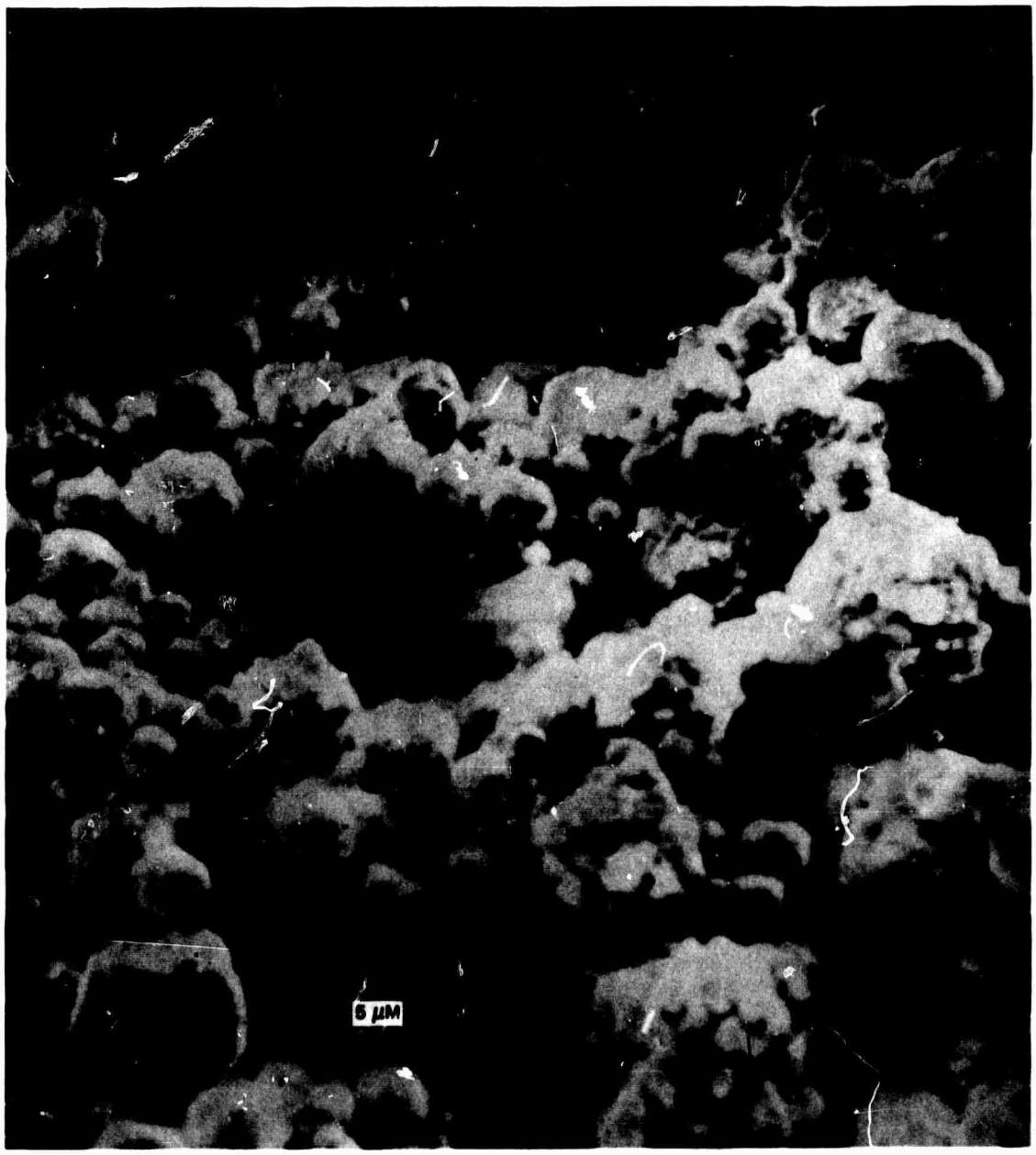

TA-8731-18

FIGURE 2 SCANNING ELECTRONMICROGRAPH OF SPHEROIDIZED Sm-Co ALLOY PARTICLE

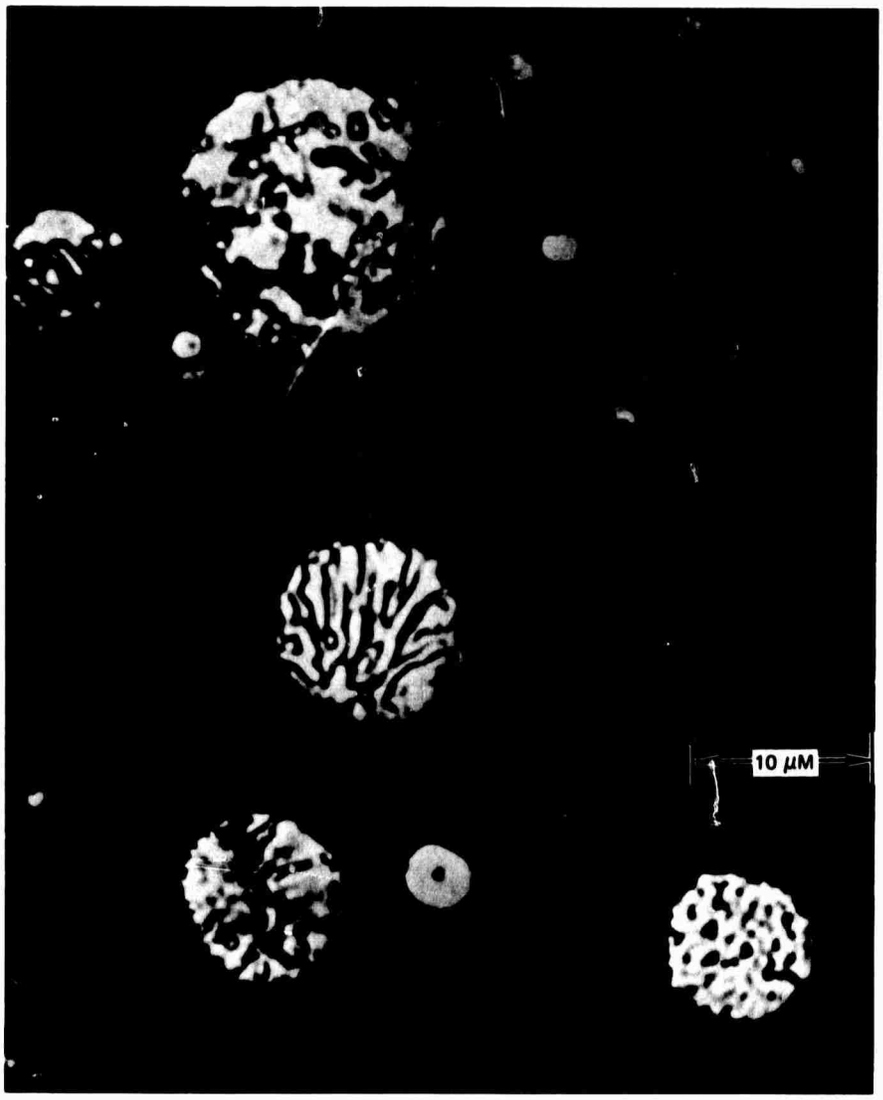

TA-8731-27

FIGURE 3 METALLOGRAPHIC CROSS SECTION OF SPHERIODIZED Sm-Co ALLOY PARTICLES (Primarily $SmCo_5$)

A second pass through the plasma gives average compositions approximately those of $RECo_5$, but these results include the fraction of the fume that is collected with the larger spherical particles.

1. Characterization of $RECo_5$ Spheroidized Alloys

An important aspect of the spheroidization study is characterization of the materials after each processing step. The samarium and praseodymium alloys with compositions near $RECo_5$ behave similarly and the history of a typical batch of material illustrates the general results and problems associated with characterizing these materials. Hence, a typical praseodymium-cobalt alloy, melt 23, will be discussed in some detail.

The stoichiometric composition of $PrCo_5$ is 32.3 wt% Pr and 67.7 wt% Co. The starting mixture of praseodymium and cobalt that was melted was 34.4 wt% Pr and 65.6 wt% Co. Weighings before and after melting showed that less than 0.1% of the material was lost during arc melting. Since the as-formulated composition contains praseodymium in excess of the $PrCo_5$ composition, the solidified button should contain Pr_2Co_7 as a second phase. The microstructure of the button from melt 23, shown in Figure 4, does show two phases.

This button was examined by electron beam microprobe (EBM) analysis, and several other analytical techniques were employed at various processing steps through plasma spheroidization. The results are summarized in Table I.

All of the analytical methods except EBM analysis give determinations that are averaged over all of the grains of the arc-melted button or all of the spherical particles and fume resulting from plasma spheroidization. Because the EBM method allows analysis of individual grains or particles, it is a critical analytical tool in this investigation.

Reported electron beam microprobe analyses are based on the ratio

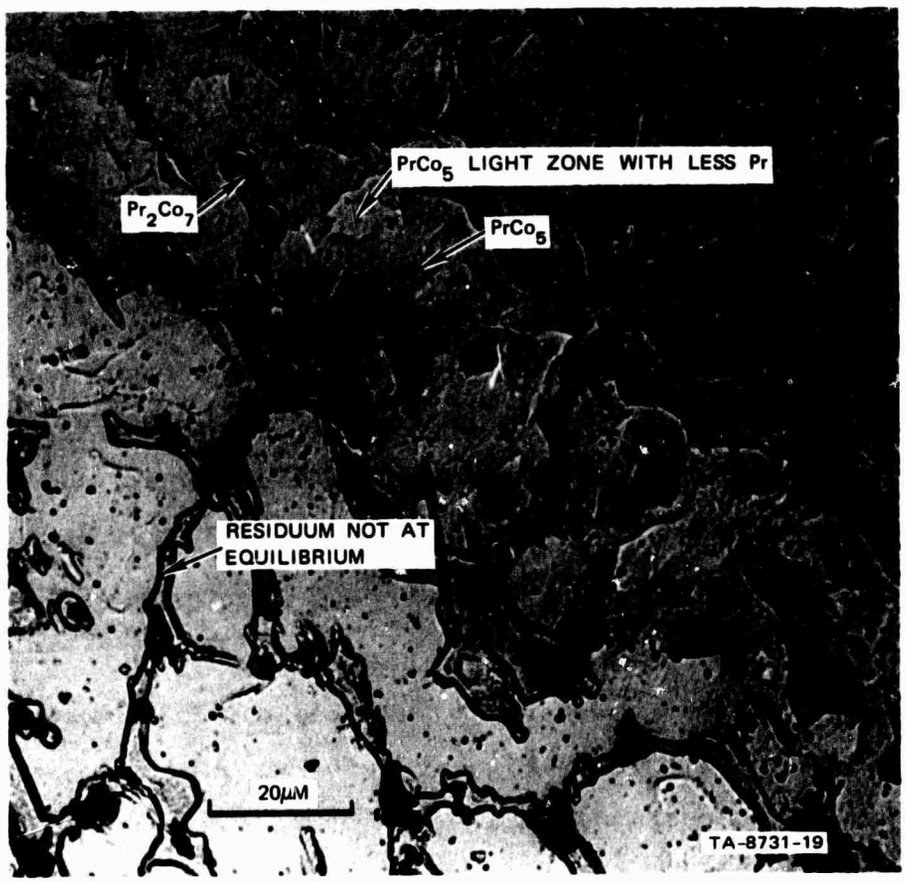

FIGURE 4 ARC MELTED $PrCo_5$ SHOWING SOME Pr_2Co_7 SECOND PHASE, MELT 23

Table I

PRASEODYMIUM COMPOSITION (wt%) OF Pr-Co MELT NO. 23

DURING PROCESSING

	Arc Melted Ingot	Spheroidized Material* Collected on Walls of Chamber
As formulated	34.4% Pr	--
Wet chemical EDTA analysis (after ball milling)	30.2%	29.9% Pr
X-ray fluorescence analysis (after ball milling)	Standard (34.4%)	29.2%
Metallographic analysis	33.3%	--
Electron beam microprobe analysis	Minor (matrix) phase (Pr_2Co_7) = 40.1% Major (dispersed) phase ($PrCo_5$) = 32.4%	(25.2%) Average for spherical particles only

*The spheroidized material contains both spherical particles (average size = 5 μm) and submicron fume.

of x-ray fluorescent intensities for the sample and a pure element standard after subtracting background intensities in both cases. No matrix absorption, atomic number, or other corrections were made.

X-ray fluorescence analyses were made in a similar manner directly on the alloys. Hence, the results can only be considered as a good first approximation of the concentrations. Furthermore, the as-formulated button concentration was used as a standard.

The wet chemical EDTA method involved dissolution of the alloy, organic extraction of cobalt, complexing of the rare earth with EDTA, and titration of the excess EDTA. On standard solutions similar to those resulting from alloy dissolution, it shows a precision of $\pm$0.1%, which is superior to that of x-ray fluorescence. Deviations on duplicate alloy samples are usually within 0.1%. This wet chemical method, which includes provision to back-extract and titrate cobalt, is described in Appendix A.

Electron beam microprobe analysis of the arc-cast material confirmed that the major phase shown in the microstructure of Figure 4 is $PrCo_5$. The minor phase results from the residual liquid after solidification of $PrCo_5$. This matrix material usually has a uniform composition, by EBM analysis, very near that of Pr_2Co_7 except when the residuum separating the $PrCo_5$ grains is exceptionally thin. In the latter instances, the peritectic reaction is evidently incomplete since there is considerable variation in composition across these zones. Figures 5 and 6 are concentration profiles across an equilibrated and a nonequilibrated region, respectively.

The average metallographic composition is based on a cumulative count of line segments of a series of randomly located straight lines crossing $PrCo_5$ and Pr_2Co_7 grains, which are easily recognized, at the surface of the metallographic section. The stoichiometric composition of these intermetallic compounds was assumed for the individual grain

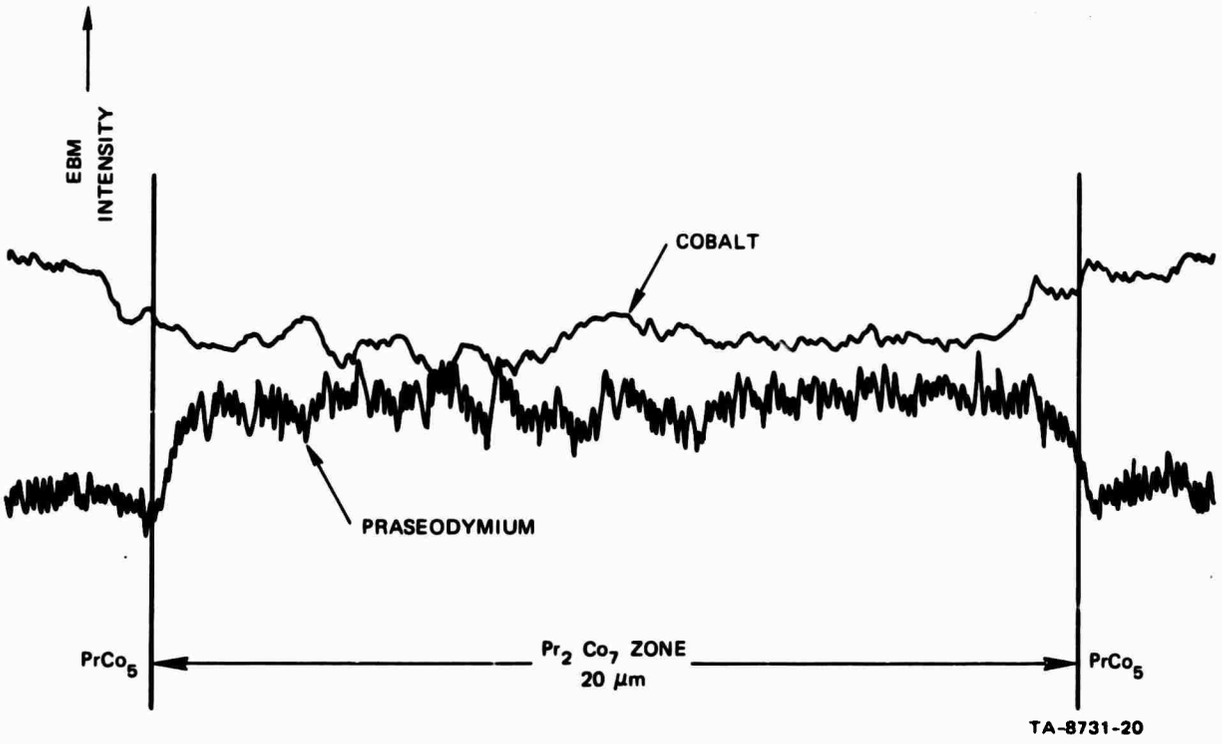

FIGURE 5 MICROPROBE TRAVERSE ACROSS EQUILIBRATED Pr_2Co_7 GRAIN FROM MELT 23

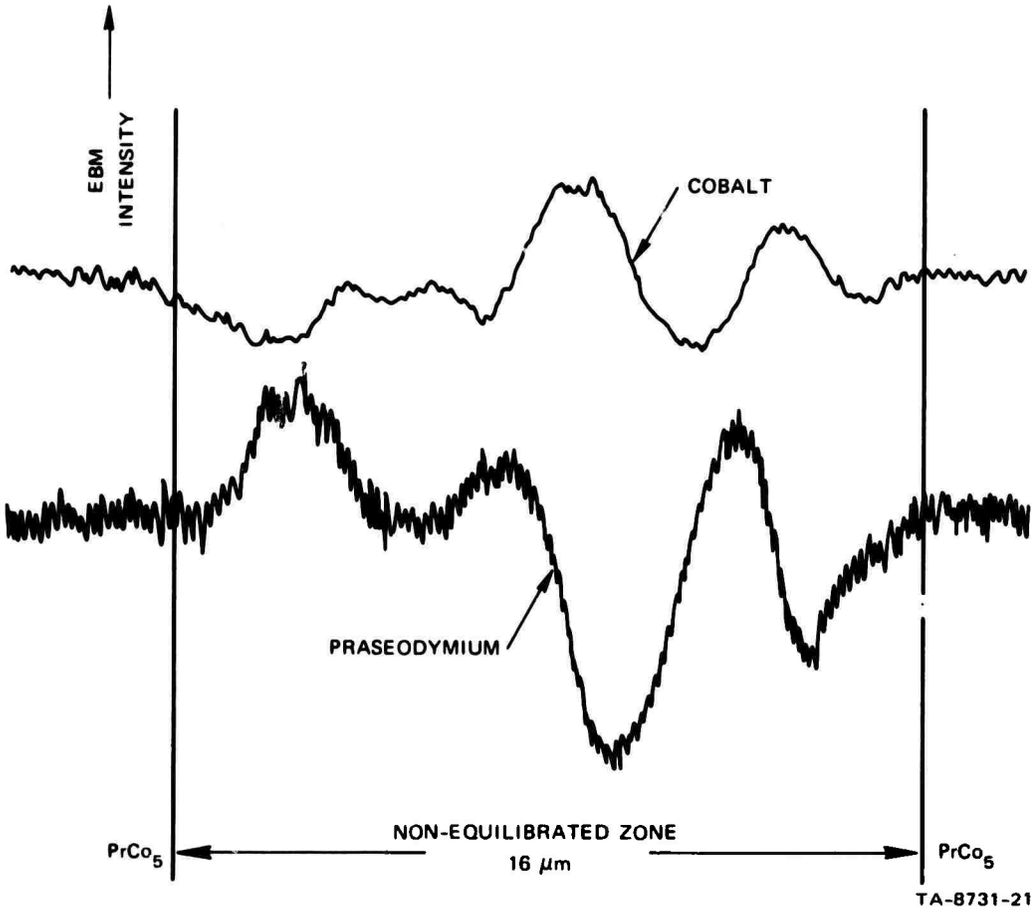

FIGURE 6 MICROPROBE TRAVERSE NONEQUILIBRATED THIN ZONE BETWEEN TWO $PrCo_5$ GRAINS IN AN ARC CAST INGOT

compositions. If the electron microprobe grain assays were substituted for the stoichiometric compositions for the major and minor phase grains, the result would not have changed much from the determined value of 33.3% Pr.

The wet chemical EDTA method reports a lower praseodymium concentration in ball-milled melt 23 than in the as-cast material. Part of this difference is attributed to dilution with debris from the alumina grinding balls. Approximately 5% of the ball-milled rare earth-cobalt alloys is insoluble, and extraction following x-ray diffraction showed this white residue to be α-Al_2O_3, the same material as the grinding balls. This amount of oxide contamination results from grinding to an average alloy particle size of about 5 μm, with substantially all of the alloy being below 20 μm. Because of this high oxide contamination further ball milling tests are being made with iron balls in alumina-lined mills, rubber-lined mills, and steel-lined mills.

The low praseodymium content of spherical particles in the spheroidized material, 25.2%, is a result of vaporization losses. Some cobalt is also vaporized, and the vaporized material condenses as a praseodymium-enriched fume. Part of the fume collects with the spherical particles on the chamber walls, causing the total average concentration by x-ray fluorescent analysis or wet chemical analysis to be higher than 25.2%. The remainder of the fume passes out of the plasma spheroidization chamber. The details of this process as it occurs for samarium cobalt alloys have been reported previously.[1]

The two phases present in arc-melted buttons with a beginning composition nearer that of $RECo_5$ than RE_2Co_7 are quite uniform in composition, with a sharp step at the phase boundary. This is illustrated by the cobalt and praseodymium microprobe traverses over a Pr_2Co_7 grain shown in Figure 5. The compositions of the phases in this alloy were 32.4% Pr and 40.1% Pr, which is close to the ideal compositions for $PrCo_5$ and

Pr_2Co_7, respectively. Light relief etching within the $PrCo_5$ field was often observed (see Figure 4), and this surface relief is associated with a small decrease in praseodymium and an increase in cobalt compared with the remainder of the $PrCo_5$ field. However, the decrease in praseodymium in the relief zone was never more than 2%. The grain sizes of both phases in the as-cast button are larger than the particle sizes of these materials after ball milling. Consequently, a bimodal composition distribution of particles is characteristic of feed materials for plasma spheroidization when the arc-melted button is off the stoichiometric composition.

X-ray diffraction patterns of melt 23 and materials after processing melt 23 were poor both before and after spheroidization and are probably a less reliable indicator of the composition of the material than are any of the methods shown in Table I. Diffraction peaks did not correspond exactly with any of the praseodymium-cobalt intermetallic compounds but could be most closely indexed to $PrCo_5$ before spheroidization, and to Pr_2Co_{17} after spheroidization. Shifting of line positions and high ratios of background to diffraction peak intensity have been the major difficulties in interpreting x-ray diffraction data. The shifting of diffraction peaks is probably caused during cooling by peritectic reactions that were incomplete.

An important aspect of any evaluation of chemical composition is the large random variation in composition of individual spheroidized particles. This information can only be obtained by EBM analysis. The variations generally observed are much greater than can be accounted for by poor EBM precision. Repeated EBM analyses of cobalt, samarium, and praseodymium standards gave results that were within $\pm 1\%$ of the mean value, with 90% of the measurements being within $\pm 0.5\%$ of the mean. This degree of precision is fairly typical of any good direct fluorescent method, including EBM analysis.

The composition variations of randomly selected particles are demonstrated by the results of EBM analyses of spherical particles in Figures 7 and 8. The data shown in Figure 8 are for a $PrCo_5$ arc-melted button (melt 22) that was closer to the stoichiometric composition than was melt 23 (Figure 7); see Table II. In both figures, the variations of praseodymium analyses are much greater than the variations of the sums of praseodymium cobalt analyses. For each particle, the cobalt variation was approximately equal and opposite to the praseodymium variation. Hence, the variations are real and not due to instrument error or caused by the electron beam overstepping a small spherical particle. In the latter instance both praseodymium and cobalt concentrations would be lowered. Melt 23 shows a greater variation of praseodymium concentrations than does melt 22, possibly because of the greater amount of second-phase Pr_2Co_7 in the feed powder.

At present, the most plausible explanation for the variation in rare earth concentration in the spherical particles is that particle residence times in the plasma are not uniform because there is considerable particle turbulence and that a greater fraction of the rare earth is lost from small particles than from large ones. Longer plasma residence times should increase the loss of the volatile rare earth element.

Table II

AS-FORMULATED COMPOSITIONS FOR BUTTONS OF ARC MELTED PRASEODYMIUM-COBALT ALLOY

	Wt% Pr	Wt% Co	Nominal Wt% $PrCo_5$	Nominal Wt% Pr_2Co_7
Melt 22	32.3%	67.6%	87%	13%
Melt 23	34.4%	65.6%	65%	35%

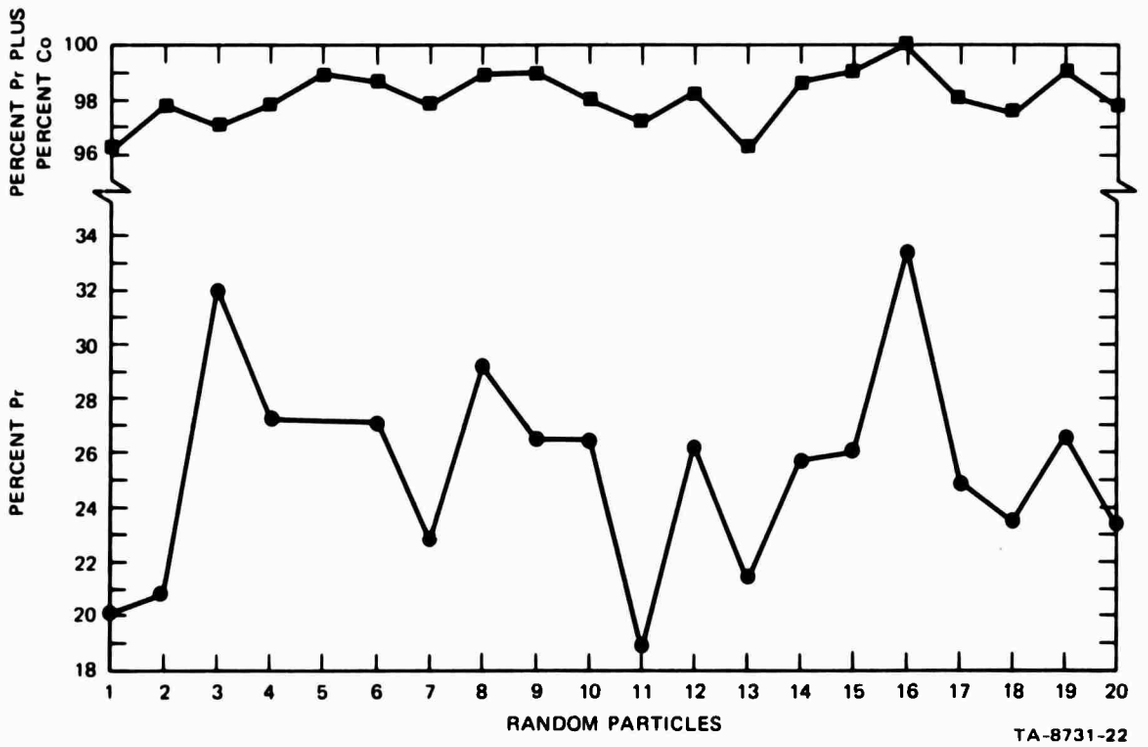

FIGURE 7 VARIATION IN PRASEODYMIUM CONTENT OF SPHEROIDIZED PARTICLES FROM MELT 23; 34.4% Pr

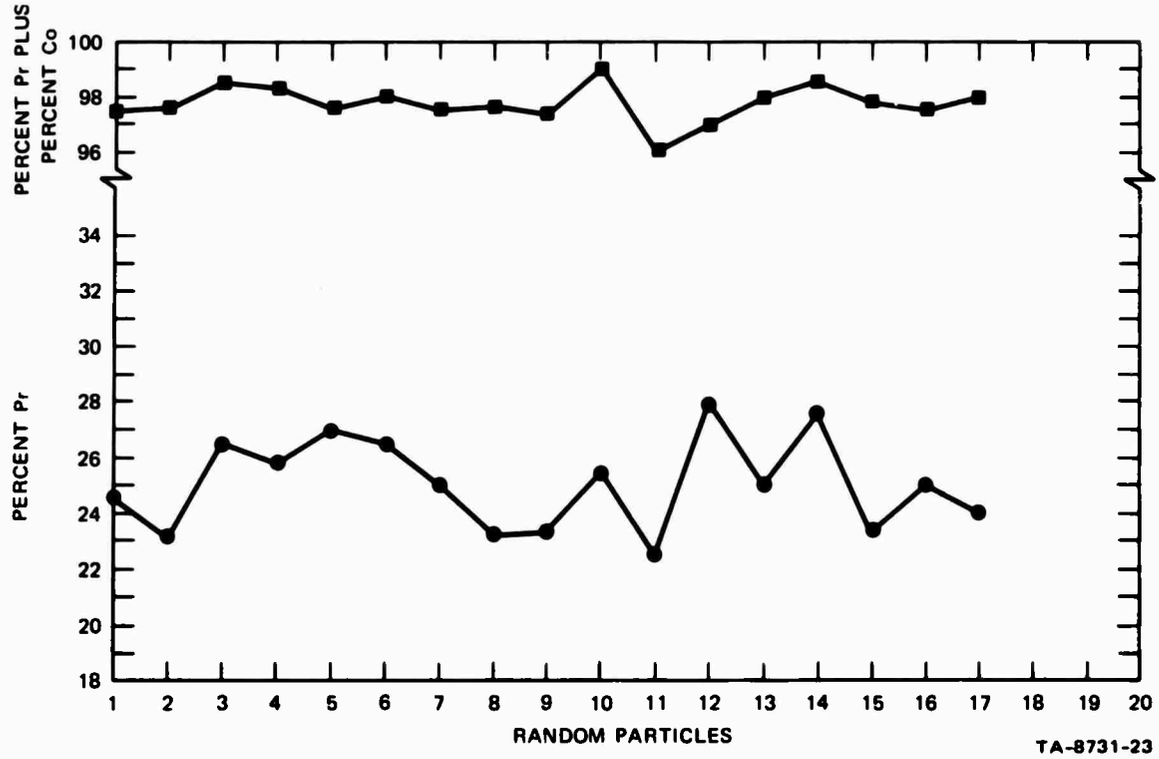

FIGURE 8 VARIATION IN PRASEODYMIUM CONTENT OF SPHEROIDIZED PARTICLES FROM MELT 22; 32.4% Pr

The characterization of spheroidized rare earth alloys is further complicated by the oxygen content. Oxygen analyses by neutron activation were made on a series of samples representing various stages in the plasma spheroidization process from the same sample lot, with an as-formulated composition of $SmCo_5$. This material was ball milled using Al_2O_3 balls.

Duplicate samples were analyzed by the U.S. Bureau of Mines, Reno, and by Gulf Radiation Technology, Inc., San Diego. Each sample was irradiated along with an oxygen standard. At Gulf Radiation Technology the samples were irradiated for 10 seconds in a 14-MeV neutron flux of approximately 18^8 neutrons/cm^2-second, and counted for nitrogen-16 induced activity on a single-channel pulse-height analyzer, using a pair of 5 x 5-inch NaI(TI) scintillation crystals. Oxygen forms N^{16} by the $O^{16}(n, p)N^{16}$ reaction. The oxygen concentration was determined by comparing the intensity of the 6.31-MeV gamma-ray photopeak of N^{16} from the sample with that from the oxygen standard.

The neutron activation oxygen analyses from both laboratories, given in Table III, are in fair agreement. Most of the oxygen content of the feed after ball milling is attributed to Al_2O_3, but oxygen is accumulated progressively by fine particles in each subsequent processing step, including room temperature storage in air. The increase of oxygen as a direct result of spheroidization is attributed to oxygen in the main argon stream to the plasma apparatus, which was not gettered with hot calcium in this particular run. The standard practice is to run all process gases over calcium chips at 625°C.

The characteristics of $SmCo_5$ alloys are similar to those of $PrCo_5$ alloys. Changes in chemical composition during processing of $RECo_5$ alloys are summarized as follows:

(1) Some rare earth is lost in arc melting 50- to 100-gram buttons--1% or less for praseodymium and about 3% for samarium.

Table III

OXYGEN ANALYSES OF STARTING MATERIALS AND $SmCo_5$ (NOMINAL) AFTER VARIOUS PROCESSING STEPS TAKEN SEQUENTIALLY FOR THE SAME LOTS OF MATERIALS

Sample	Gulf Oxygen Analysis	USBM Oxygen Analysis
Distilled lump samarium (starting material)	454 ppm ± 84	700 ppm
Cobalt shot (starting material)	377 ppm ± 48	520 ppm
Arc melted and ball milled $SmCo_5$ particles (feed)	1.50 wt% ± 0.059	1.71 wt%
Spheroidized particles	2.82 wt% ± 0.110	3.59 wt%
Spheroidized particles after 24 hours storage in air	5.07 wt% ± 0.210	5.10 wt%
Spheroidized particles after 24 hours storage in air and removal of the -20 micrometer particles by sieving	3.72 wt% ± 0.150	3.41 wt%

(2) The grains of $SmCo_5$ and $PrCo_5$ in arc-melted buttons are of the correct stoichiometric composition.

(3) Excess praseodymium (or samarium) is rejected as Pr_2Co_7 (or Sm_2Co_7), but the grains of this phase are not always equilibrated after arc melting.

(4) Praseodymium and cobalt concentrations are lowered because of dilution with the grinding media (Al_2O_3, ~5%).

(5) Plasma spheroidization causes loss of praseodymium (or samarium) by vaporization from the spherical particles and condensation of a praseodymium-rich (or samarium-rich) fume. The loss of rare earth varies considerably from particle to particle.

(6) Oxygen contamination is due primarily to the grinding media prior to spheroidization. The plasma-treated product is very reactive to oxygen, and this is probably due to reaction with the submicron fume rather than with the 1- to 20-μm spherical particles. Electron beam microprobe oxygen analysis of fume and spherical particles support this contention.

(7) The best analytical methods available for chemical characterization are as follows:

Element	Bulk Samples (Average)	Individual Particles
Rare Earth	Wet chemical EDTA titration	Electron beam microprobe
Cobalt	Wet chemical after organic extraction	Electron beam microprobe
Oxygen	Neutron activation	Electron beam microprobe

2. Characterization of RE_2Co_7 Spheroidized Alloys

Both $RECo_5$ and RE_2Co_7 are produced on cooling by a peritectic reaction between a solid phase and the residual liquid. For the samarium and praseodymium alloys the difference between liquidus and peritectic temperatures is much greater for RE_2Co_7 than for $RECo_5$; consequently, the RE_2Co_7 peritectic reaction is much more sluggish than the $RECo_5$ peritectic reaction. During solidification of liquid compositions at Sm_2Co_7 or between Sm_2Co_7 and $SmCo_5$, the $SmCo_5$ solid is formed initially. During arc melting and solidification of 50- to 100-gram buttons, the rate of cooling on the cold copper hearth is too fast for the peritectic reaction between $SmCo_5$ and excess liquid to occur to any significant degree. The resulting x-ray diffraction patterns are very poor but somewhat closer to those of $SmCo_5$ than to those of Sm_2Co_7.

The microstructure resulting after arc melting Sm_2Co_7 is shown in Figure 9. From electron beam microprobe analyses this alloy is known to be chemically inhomogeneous. After annealing at 1000°C, or higher temperatures, for one hour under argon, the alloy has a similar microstructure, but microprobe traverses show that it is homogeneous, with the composition and x-ray diffraction spectra of Sm_2Co_7. Heating arc-melted Sm_2Co_7 ground particles at low temperatures, 300° to 400°C, where sintering does not occur had no homogenizing effect. Fortunately, annealing arc-melted Sm_2Co_7 ingots at 1000°C prior to grinding is a satisfactory method for producing homogeneous Sm_2Co_7 particles.

In plasma spheroidizing cobalt alloys of samarium and praseodymium, it is necessary to start with a single-phase homogeneous alloy ingot, since grinding is extended to particle sizes smaller than the ingot grain size. If the original ingot contains two phases, then a bimodal composition distribution of fine particles will result after grinding. Regardless of the operating controls imposed during spheroidization, the resulting spherical

FIGURE 9 ARC MELTED Sm_2Co_7

particles will have differing compositions because of their different starting compositions. To produce single-phase spherical particles ($RECo_5$), it is necessary to start with a single-phase particle (RE_2Co_7) and vaporize the correct amount of rare earth element required to shift the composition from the RE_2Co_7 phase field to the $RECo_5$ phase field.

Two passes of Sm_2Co_7 particles through the plasma at 15 kw and standard operating conditions provide particles with a composition approximately that of $SmCo_5$. Since some of the fume is collected with the spheroidized particles, it is not possible to determine the average composition of the larger spherical particles separately from the fume.

The x-ray diffraction pattern resulting from single and double plasma spheroidization is extremely poor. It appears that some of all three phases, Sm_2Co_7, $SmCo_5$, and Sm_2Co_{17}, are present, but a definite conclusion cannot be made from x-ray diffraction data. Because of rapid droplet cooling and vaporization of samarium, the resulting spherical particles may be inhomogeneous and strained.

C. Plasma Heat-Treated $RECo_5$ Particles

The argon plasma has also been used to heat $SmCo_5$ and $PrCo_5$ particles to high temperatures without exceeding their melting points. The plasma provides a relatively noncontaminating atmosphere where the hot particles are not in contact with each other and cannot sinter. Possible advantages of this heat treatment include relief of internal stresses in the comminuted particle. removal of surface oxides when the heat treating is conducted in an atmosphere containing a sufficiently reducing vapor such as samarium or calcium, and removal of surface layers by hot gas etching.

Two types of experiments have been performed. In the first type of experiment, previously comminuted powders of $SmCo_5$ and an enriched

samarium-cobalt eutectic alloy have been well mixed and injected into the plasma torch at low power setting where only the eutectic particles melt. Since the eutectic particles contain a high proportion of samarium considerable samarium vaporization occurs when they melt and this tends to inhibit oxidation of the magnet alloy particles. Plasma annealing previously spheroidized particles was also investigated. Particles of the eutectic alloy were included to inhibit oxygen contamination.

In the second type of experiment, chlorine was included with argon in the particle carrier gas and injected in a low-power plasma where particle melting does not occur. At elevated temperatures, chlorine will react with both samarium and cobalt to yield volatile chlorides. The chlorides of these metals have been collected from the downstream gases and the surface texture of the particle changes, indicating that chlorine does etch the particle surface during its short exposure in the plasma.

D. Magnetic Evaluation of Plasma-Treated Particles

The intrinsic coercive forces of the rare earth-cobalt alloy powders produced during this study were measured using a Princeton Applied Research vibrating magnetometer coupled to a 75-kilogauss superconducting magnet. A description of the specimen preparation procedure is given in Appendix B. The results are summarized in Table IV.

The $SmCo_5$ alloys that had been ball milled for 3 hours, average particle size 5-10 microns, had intrinsic coercive forces above 20,000 oersteds if they were not exposed to air prior to being set in the epoxy binder. Specimens were magnetized with fields of 50,000 oersteds before measurement. Prolonged exposure of the loose powder to air at room temperature lowered the intrinsic coercivity by about 10%.

Table IV

SUMMARY OF MAGNETIC EVALUATIONS OF PLASMA SPHEROIDIZED AND ANNEALED PARTICLES

Run	Material	Starting* Composition	Power (kw)	H_m (kOe)	H_c (Oe)	$4\pi M_r$ (G)	Remarks
Ball-Milled Samples							
M27	Sm_2Co_7	47.5% Sm 52.5% Co		35	11,100	5160	As ground, ball milled 3 hours
M28	$SmCo_5$	36% Sm 64% Co		50	20,300	8000	As ground, ball milled 3 hours
M29A	$SmCo_5$	15% (84% Sm, 16% Co)† 85% (36% Sm, 64% Co)		53	16,250	5640 †† (8650)	As ground, ball milled--left in air for one week before epoxy binding
M33	$SmCo_5$**	36% Sm 64% Co		50	22,000	8775	As ground, ball milled 3 hours
Plasma Spheroidization							
P3	$SmCo_5$			35	700	--	
P21	$SmCo_5$	85% (36% Sm, 64% Co) 15% (84% Sm, 16% Co)	12.0	55	5,640	--	
P16		44.75% Sm 55.25% Co	15.5	35	9,650	--	Epoxy cured at 70°C (normal cure is at room temperature)
P17	$PrCo_5$	32.4% Pr 67.6% Co	15.5	35	1,070	2800	Sample was exposed to air and possible oxidation
P18	$PrCo_5$	32.4% Pr 67.6% Co	15.5	35	1,800	3250	Epoxy cured at 70°C
P20		44.75% Sm 55.25% Co	15.5	35	3,750	2960	
P27		47.5% Sm 52.5% Co	15.5	51	8,350	5070	Powder feed <400 mesh, was hand ground rather than ball milled to limit extremely fine particles
P28		47.5% Sm 52.5% Co	15.5	52	4,000	3020	Sample exposed to air
P31	$SmCo_5$	15% (84% Sm, 16% Co) 85% P28 residue	15.5	53	4,400	3090	Plasma spheroidization using spheroidized material from Run P28
Plasma Annealed							
P10	$SmCo_5$	36% Sm 64% Co	5.0	35	2,500	--	
P22	$SmCo_5$	85% (36% Sm, 64% Co) 15% (84% Sm, 16% Co)	5.5	53.5	11,500	--	Injected powder into the middle of the plasma
P23	$SmCo_5$	85% (36% Sm, 64% Co) 15% (84% Sm, 16% Co)	5.5	53	11,900	7310	Injected powder into bottom of plasma
P24			5.5	53	14,000	--	Injected powder below plasma
P26	$SmCo_5$	15% (84% Sm, 16% Co) 85% (36% Sm, 64% Co)	5.5	53	13,900	7680	
P30	$SmCo_5$	15% (84% Sm, 16% Co) 85% P28 residue	5.5	51	11,800	7870	Plasma anneal using material from Run 28
P32	$SmCo_5$	15% (84% Sm, 16% Co) 85% P31 residue	5.5	50	4,140	2570	Run P31 annealed after spheroidization
Chlorine Etch							
P25	$SmCo_5$	36% Sm 64% Co	5.5	54	7,400	--	Plasma annealing in Cl flowing at 120 cc/min through particle feeder
P25	$SmCo_5$	36% Sm 64%	5.5	50	3,300	5830	Plasma annealing in Cl flowing at 600 cc/min through particle feeder

*Some rare earth is lost by vaporization in arc melting and plasma spheroidization.

**Sharpest x-ray diffraction pattern for $SmCo_5$ obtained is arc-melted alloys.

†Low-melting near-eutectic alloy composition containing mostly samarium.

††Adjusted for dilution by eutectic alloy.

Plasma spheroidization of milled $SmCo_5$ material resulted in spherical particles containing a second phase, Sm_2Co_{17}. The intrinsic coercivities were approximately 1000 oersteds. When excess samarium was included as separate particles with a $SmCo_5$ particle feed, loss of samarium was evidently suppressed, and in run P21 the intrinsic coercivity was 5640 oersteds. The intrinsic coercive force was also increased when the starting particles had excess samarium, $\sim Sm_2Co_7$. The highest intrinsic coercivity on this material after spheroidization was 9650 oersteds, following magnetization with a field of 35,500 oersteds. $PrCo_5$ materials also exhibit lower coercivities following plasma spheroidization.

Annealing the $SmCo_5$ particles without melting them provided higher coercive forces than plasma spheroidization but less than obtained with simple comminution. Plasma annealing 15 wt% enriched Sm eutectic particles with 85 wt% $SmCo_5$ particles resulted in an intrinsic coercive force of 13,900 oersteds at the lowest plasma heating rate. Cycling the $SmCo_5$ particles through the plasma to extend the annealing time resulted in decreased coercivities. The results generated from this sequence of experiments are summarized in Table V.

Table V

EFFECT OF PLASMA ANNEALING ON THE COERCIVITY OF $SmCo_5$ POWDERS

Material	H_{mc}, oersteds
As ground $SmCo_5$	20,300
After Room temperature aging one week	18,250
After First cycle plasma anneal	13,900
After Second cycle plasma anneal	11,800

Chlorine was introduced into the plasma in an attempt to produce gaseous chemical removal of the surface of the $SmCo_5$ particles, which may improve the coercivity of the material. Using a chlorine flow rate of 120 cc/min mixed with the feed gas resulted in samarium-cobalt particles having coercivities of 7400 oersteds. Increasing the chlorine flow rate to 600 cc/min caused a decreased coercivity of 3300 oersteds.

The data presented in this section indicate that oxygen contamination of the $SmCo_5$ particles causes a greater loss in the intrinsic coercive force than is gained by any possible annealing or spheroidization of the $SmCo_5$ particles.

The values of $4\pi M_r$ shown in Table IV do not contain any corrections for demagnetization effects nor corrections for possible nonuniformity in the sample magnetization. It is believed that these effects are small in those samples exhibiting the best magnetic properties; this premise will be checked in future experiments. Spheroidization also lowers the magnetic remnance and the magnetization generally. This results because individual grains are not always single unattached crystals that can be uniformly aligned in a magnetic field. Plasma spheroidization that results in the production of either Sm_2Co_7 or Sm_2Co_{17} as a second phase in the $SmCo_5$ particles also lowers $4\pi M_r$ as expected.

The data shown in Table IV show that plasma annealing of $SmCo_5$ does not significantly affect the value of $4\pi M_r$. However, the intrinsic coercive force, $_mH_c$, of $SmCo_5$ powders decreases with each plasma heat treatment.

III ALTERNATIVE METHODS OF PARTICLE PREPARATION

A variety of processes for preparing rare earth-cobalt alloy particles other than simple grinding and plasma spheroidization were investigated. The primary goal of this research was to determine what methods, if any, would produce particles with a higher magnetic coercivity than comminuted particles. The study was confined to cobalt alloys of samarium and praseodymium. The processes investigated were electrolysis in fused salts, electrolysis at room temperature in organic liquids, chemical reduction from acetate solutions into a falling amalgam droplet, precipitation from a distilling liquid zinc solution, and direct reduction of cobalt chloride with the samarium-cobalt eutectic alloy. None of these methods has yet produced higher magnetic coercivities than can be achieved by simple grinding. Some of them have been discarded while others are not yet adequately evaluated.

A. Electrolysis in Fused Salts

Four electrolysis experiments were conducted at 950°C in a cold wall vacuum furnace with a graphite resistance heating element and molybdenum radiation shields. Fused anhydrous fluorides were used as the electrolyte, and molybdenum crucibles were used as the electrolyte containers. For each experiment the furnace chamber was evacuated to below 10^{-5} torr and baked. Calcium gettered argon was flowed through the system at a pressure slightly over 1 atm while the electrolyte was melted and the electrolysis experiment was conducted. The use of an argon atmosphere reduced the vaporization of the electrolyte constituents that would have occurred in vacuum. These experiments are summarized in Table VI.

Table VI

SUMMARY OF FUSED SALT ELECTRODEPOSITION EXPERIMENTS

Run	Anode	Cathode	Electrolyte	Floating Potential Electrode	Temp. °C	Voltage	Current Density amps/cm^2	Cathode Deposit	Change in Electrolyte Composition	Changes in Floating Potential Electrode	Remarks
DC-8	Molybdenum	$SmCo_5$	59% BaF_2 41% LiF (eutectic)	Sm (30 wt% of electrolyte)	950°C	0.2	0.6	Lithium	Includes Sm^{++}	Not analyzed but melted	Electrodes bridges and shunted
DC-11	Molybdenum	$SmCo_5$	50% SmF_2 20% BaF_2 30% LiF	Sm (30 wt% of electrolyte)	950	~0.5	4.0	Samarium	--	Includes cobalt and melted because the liquidus temperature was lowered by cobalt	Constant current
DC-12	Molybdenum	$SmCo_5$	59% BaF_2 41% LiF (eutectic)	Sm (30 wt% of electrolyte)	950	0-0.5	0-4	Lithium	Includes Sm^{++}	Includes cobalt and melted because the liquidus temperature was lowered by cobalt	Variable current and voltage
DC-17	Molybdenum	$SmCo_5$	50% SmF_2 20% BaF_2 30% LiF	None	950	1.0-2.4	4.0	Massive deposit; Sm/Co = 4.0 by weight--but contained other impurities	None--$[Sm^{++}]$ remained constant and $[Co^{++}]$ was below detection limits	(Not applicable)	Constant current (conductivity decreases when free samarium is not present in the electrolyte

Molybdenum cathodes and $SmCo_5$ anodes were used. The anodes were formed by melting and solidifying $SmCo_5$ in pyrolytic boron nitride crucibles. The melting was done in a vacuum furnace with the crushed $SmCo_5$ outgassed at 750°C before introducing the gettered argon cover gas and melting. The electrolyte was prepared by mixing nominally anhydrous salts in powder form, baking in vacuum to remove water, melting in gettered argon, and heating to 950°C. After they were cooled to room temperature, the solid electrolyte salt plugs were removed from the furnace and stored in a glove box while awaiting the electrolysis experiment.

Two of the experiments involved a 60 wt% BaF_2-40 wt% LiF electrolyte (eutectic mixture). An excess of metallic samarium, 30 wt% of the electrolyte, was added to the electrolysis cell to saturate the electrolyte with dissolved neutral samarium. As reported earlier[1] this fused salt mixture dissolves considerable samarium on heating, and the samarium reprecipitates as metallic samarium on cooling. The samarium added to the electrolytic cells was in the form of coarse crushed lumps that settled in the cell. This constitutes a third electrode and source of samarium at a floating potential. Electrolysis was carried out using a current-regulated power supply. The voltage across the cell was measured, and in one of these experiments current was varied over a wide range to a maximum of 10 amperes, corresponding to an electrode current density of approximately 3 to 4 amperes/cm^2. The uncertainty in current density results from the irregular electrode surface. The results of this experiment are plotted in Figure 10. The voltage across the cell is proportional to

[1] AFML-TR-71-30, Semiannual Report, p. 24

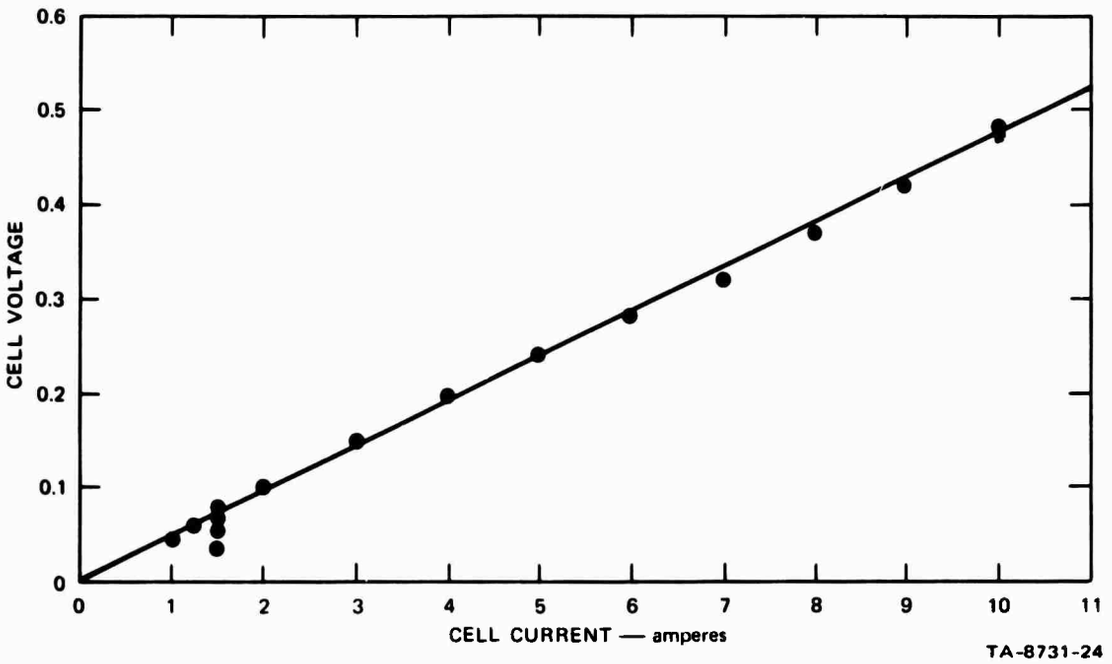

FIGURE 10 CELL VOLTAGE-CURRENT RELATION FOR ELECTROLYSIS OF 60% BaF_2-40% LiF USING A $SmCo_5$ ANODE AT 950°C

current density, indicating that electrical resistance of the electrolyte, rather than a nonlinear electrode polarization phenomenon, accounts for the cell voltage. This result is consistent with the reversible electrochemical behavior of most fused salt electrolysis systems, even at high current densities. The anode corroded fairly uniformly, but neither samarium nor cobalt was deposited at the cathode. Lithium was deposited at the cathode, and some of this evaporated from the cell while the remainder dripped off the cathode and formed an alloy with the samarium in the bottom of the cell. Analysis of the residual electrolyte showed samarium but not cobalt. Hence, both samarium and cobalt were oxidized at the anode, the samarium ions remained in the electrolyte, and cobalt ions were immediately reduced by the soluble neutral samarium in the electrolyte. The reduced cobalt was then alloyed with the excess samarium in the bottom of the cell, forming a liquid at the operating temperature. Note the steep liquidus curve at the samarium-rich end of the samarium-cobalt phase diagram, Figure 1. If the cell had been run for a longer time so that the activity of samarium ions at the cathode was sufficiently increased, samarium rather than lithium would have been deposited. This was shown by experiment DC-11, involving a high concentration of samarium ions in the electrolyte.

The electrolyte used in the run DC-11 contained 50 wt% SmF_2, 30 wt% BaF, and 20 wt% LiF. A 30 wt% excess of neutral samarium was also used. The cell configuration was similar to that of the previous experiments, with a cell voltage of about 0.5 volt at 10 amperes. The current was held constant and the cell voltage decreased somewhat with time. Samarium was deposited at the cathode while the dissolved cobalt ions were again reduced by samarium in the salt and formed a

liquid alloy with samarium in the bottom of the crucible. The $SmCo_5$ anode corroded uniformly with respect to its chemical composition. The cathode and anode are shown in Figure 11.

It was concluded from the first three experiments that cobalt is oxidized at the anode along with samarium, but as cobalt ions diffuse from the anode they are immediately reduced by the neutral samarium dissolved in the electrolyte. The reduced cobalt, or cobalt-samarium alloy, precipitates and drops to the bottom of the cell, where dilution with additional excess samarium occurs forming a cobalt-samarium liquid alloy phase in the general composition region near the alloy eutectics, 10 to 40 atomic pct cobalt. Hence, cobalt cannot be transferred to the cathode when neutral samarium is added to the cell, and in the fourth experiment, DC-17, samarium was not included. This experiment ran the risk of redissolving into the electrolyte any samarium deposited at the cathode, but it avoided the direct reduction of Co^{++} by excess Sm^{o} in the electrolyte.

The cathode deposit for run DC-17 contained both cobalt and samarium, but more samarium than would correspond with dissolution of the $SmCo_5$ anode. This result indicates that some net electroreduction of Sm^{++} ions from the electrolyte occurred. This experiment was conducted with a constant current. The cell voltage increased from 1.0 to 2.4 volts during the one-hour electrolysis period. The dissociation potential of this electrolyte to yield samarium is unknown and cannot be estimated from the free energy of decomposition of SmF_2, which is also undetermined. The decomposition potential of pure LiF is 2.2 volts at 1000°C; the decomposition potential of pure BaF_2 is 2.58 volts at 1400°F.[2] The decomposition potential of SmF_2 should be slightly less than that for LiF. It should be noted that

[2] Yu.K. Delimarskii and B. K. Markov, Electrochemistry of Fused Salts, R. E. Wood, ed., Chap. 3 (Sigma Press, Washington, D.C., 1961).

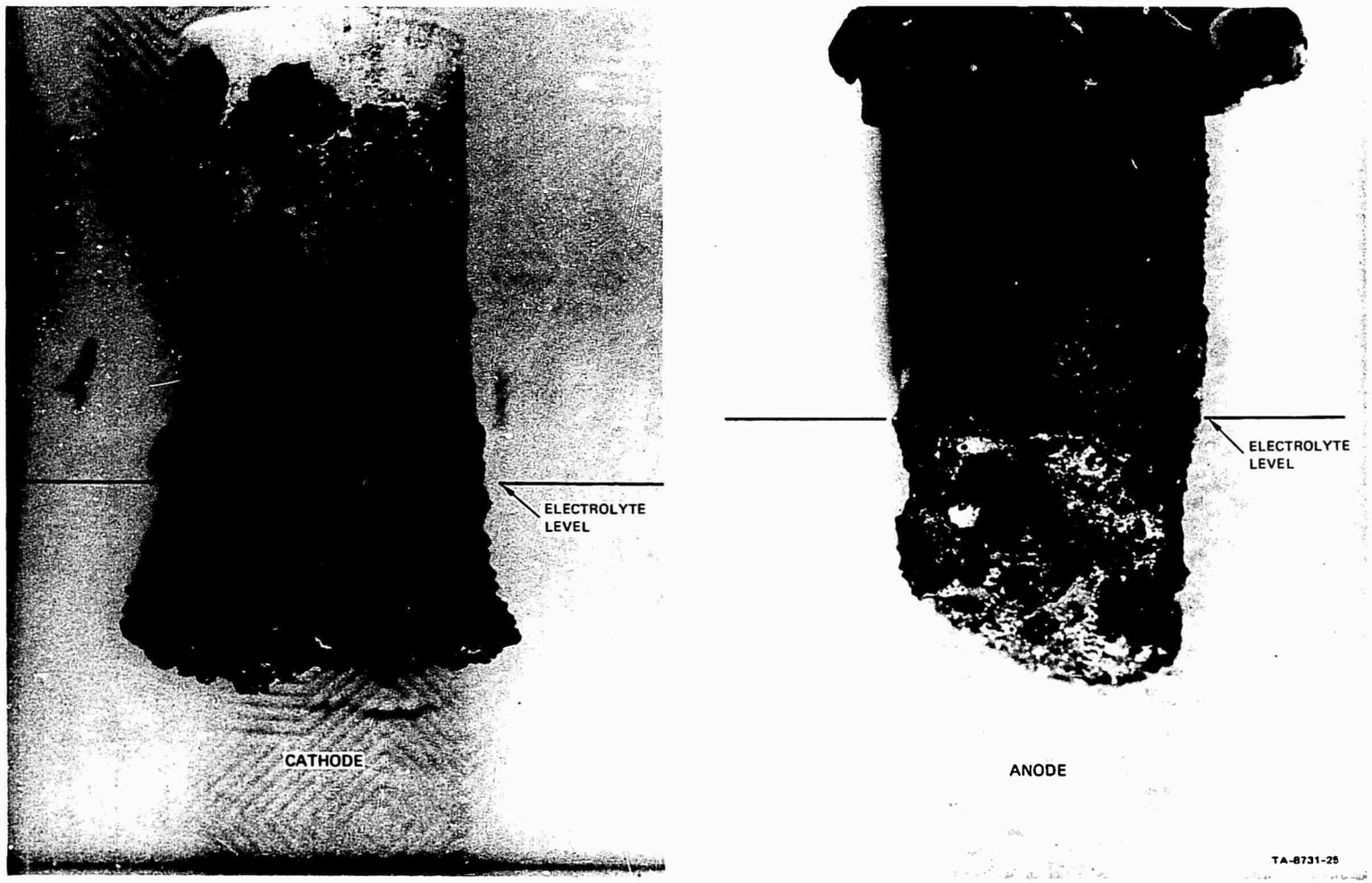

FIGURE 11 SAMARIUM DEPOSIT ON CATHODE AND $SmCo_5$ ANODE AFTER ELECTROLYSIS IN 50% SmF_2-30% BaF_2-20% LiF

both SmF_2 and SmF_3 are stable compounds, whereas praseodymium forms only one stable fluoride, PrF_3. However, in the presence of metallic samarium or one of its alloys, SmF_2 is expected rather than SmF_3.[3]

The cathode deposit from run DC-17 was smooth and massive and appeared to have partially melted at the surface after deposition. This can be explained if the samarium/cobalt ratio in the electrodeposit increased as the cell voltage increased during the electrolysis experiment due to net decomposition of SmF_2 in the electrolyte. If the Sm/Co ratio increases from valves initially near that of $SmCo_5$, the liquidus temperature will decrease (see Figure 1). Melting would have occurred at the cell operating temperature of 950°C if the Sm/Co weight-ratio had decreased to 3.3. If the electrodeposit has a uniform composition with a liquidus temperature below the cell temperature, none of it should have been retained on the cathode. The cobalt containing electrodeposit is magnetic but does not have superior properties. An electrodeposited alloy of $SmCo_5$ is required before improved magnetic coercivities can be expected.

Further fused salt electrolysis experiments will be conducted at cell potentials well below the range of decomposition of SmF_2 in an attempt to obtain an electrodeposit of correct stoichiometry.

B. Electrolysis in Organic Liquids

Electrolytic experiments have been conducted at room temperature with nonaqueous electrolytes. Polar organic solvents containing dissolved inorganic salts have been used as the electrolytes, and mercury has been used as the cathode. A simple schematic drawing of the cell is shown in Figure 12.

---

[3] D. Brown, Halides of the Lanthanides and Actinides, p. 86. (Wiley-Interscience, New York, 1968).

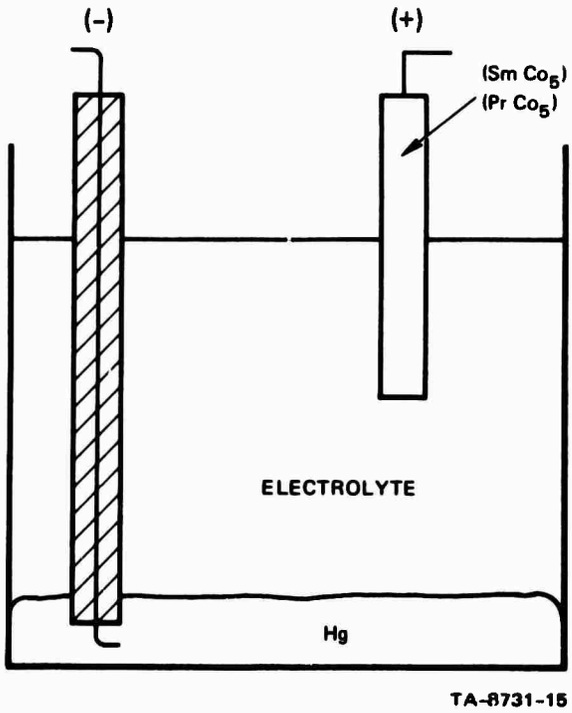

FIGURE 12 SKETCH OF THE NONAQUEOUS ELECTROLYTIC CELL

Electrolyte materials were prepared as follows: All solvents were dried by passing the solvent over a column (35 mm x 2.5 cm OD) of molecular sieves, Type A. The solvents were collected under dry nitrogen and stored over molecular sieves in a drybox. The molecular sieves were activated by heating at 200°C under vacuum overnight. Lithium perchlorate was dried by heating the salt to just below its melting point (235°C) for 16 hours, and finally melting the salt under vacuum. Dry lithium tetra-fluoroborate was synthesized in our laboratory. Magnesium perchlorate was dried by heating the salt at 120°C in vacuum. Other perchlorate salts were prepared from samarium metal and from the samarium-cobalt alloy and dried in a vacuum oven at 60°C.

After electrolysis, mercury was removed by vacuum distillation in a quartz vessel from the electrolysis product formed at the cathode. The presence or absence of rare earth in the product was confirmed by dissolving some of the electrolysis product in 3N hydrochloric acid and making the resulting solution strongly alkaline with ammonium hydroxide. The presence of rare earth metal is noted by the formation of a flocculent gelatinous precipitate.

The results of experiments performed under various conditions are summarized in Table VII. In all of the electrolyses using samarium and $SmCo_5$ anodes, deposition appeared to take place at the cathode, but a black deposit containing samarium formed on the surface of the mercury cathode soon after electrolysis began. This samarium residue is believed to have formed by back reaction of the samarium amalgam with the solution. When a lithium salt was included in the electrolyte, a lithium amalgam formed during electrolysis.

Table VII

SUMMARY OF CONDITIONS AND RESULTS OF ORGANIC ELECTROLYSIS EXPERIMENTS

Experiment No.	Electrodes		Electrolyte			Applied Voltage & Current		Reaults and Remarka
	Anode	Cathode	Solvent	Salt	g/l	V (Volta)	I (mA)	
1	Sm-Co_5 alloy	Platinum foil	Propylene carbonste	$LiClO_4$	160	50	10-20	Electrolyzed material was a mixture of cobalt and lithium metal. No samarium was observed by qualitative testa.
2	Sm-Co_5 alloy	Platinum foil	Propylene carbonate	$Mg(ClO_4)_2$	20	50	5-10	Thin film of cobslt metal was obtained.
3	Sm-Co_5 alloy	Platinum foil	Acetone	$LiClO_4$	160	10	50-250	X-ray diffraction ahowed a mixture of aamarium and cobalt oxides. Qualitative analysia did not confirm the presence of samarium. The product waa a powder and was very magnetic.
4	Sm-Co_5 alloy	Platinum foil	Acetone	$SmCo_5$ perchlorate	20	10	10	Some cobalt metal was obtained No positive evidence of samarium being present in product.
5	Pt wire	Hg pool	Acetone	$SmCo_5$ perchlorate	10	50	50-250	Magnetic powder obtained after atripping off Hg. Qual. anal. ahowed absence of aamarium.
6	Pt wire	Hg pool	Acetone	$SmCo_5$ perchlorate	10	10	50-250	Same as Experiment No. 5.
7	Pt wire	Hg pool	Methanol	$SmCo_5$ perchlorate	50	10	100	Same as Experiment No. 6.
8	Pt wire	Hg pool	Propylene carbonate	$Sm(ClO_4)_3$	Sat'd	25	40	No aamarium metal was obtained after removing the mercury.
9	Pt wire	Hg pool	Propylene carbonate	$SmCo_5$ perchlorate	Sat'd	40	180	Same as Experiment No. 7.
10	Sm-Co_5 alloy	Hg pool	Propylene carbonate	$SmCo_5$ perchlorate	43	28	105	Weakly magnetic powder obtained, but qual. anal. did not confirm preaence of aamarium.
12 & 13	Sm-Co_5 alloy	Hg pool	Propylene carbonate	$SmCo_5$ perchlorate	664 Sat'd	6	40	Strongly magnetic particles obtained but qual. examination showed the absence of aamarium
14	Pt wire	Pt foil	Acetone	Samarium perchlorate	Sat'd	10	20	No samarium metal electrolyzed out. Gelatinous yellow material plated out at the cathode
15 & 16	Sm-Co_5 alloy	Hg pool	Propylene carbonste	$SmCo_5$ perchlorate	26	20	20	Magnetic particles obtained; qual. evidence of aamarium waa negative.
17 & 18	Sm metal	Hg pool	Dimethyl sulfoxide	$LiClO_4$	7	130	20	Approximately 100 mg of a material was obtained. Thia material did not amalgamate with the mercury. The residue left after distillation of the mercury was nil. Alao, the aamarium appears to enter and come out of the mercury very rapidly. Samarium metal waa absent in the residue from the Hg diatillator.
19 & 20	Sm metal	Hg pool	Aceto-nitrile	$LiBF_4$	6	14	100	A black material collected on top of the mercury pool. No metallic aamarium waa obtained in the mercury cathode.
21	Cobalt metal	Sat'd samarium amalgam	Aceto-nitrile	$LiBF_4$	36	25	500	Black magnetic powder waa obtained. Qual. exam. showed a small amount of aamarium to be present.
22	Praseo-dymium Cobalt metal	Hg pool	Aceto-nitrile	$LiClO_4$	53	E_{Pr}= 9V E_{Co}=50V	I_{Pr} = 2 mA I_{Co} =15mA	A small amount of magnetic material was obtained which did not contain praseodymium.
23	Pr metal	Hg pool	Aceto-nitrile	$LiBF_4$	30	20	175	The reaulting amalgam contained both lithium and praseodymium metal. No black deposits formed on the aurface of the mercury cathode.

One experiment was conducted in an electrochemical cell consisting of two isolated anode compartments, one with a praseodymium anode and the other with a cobalt anode, with a common mercury cathode compartment. The mercury was stirred manually during electrolysis.

In summary, the following was shown: (1) cobalt is electrolyzed easily into a mercury cathode (or onto a platinum cathode); (2) the electrolysis product after mercury removal by distillation is friable; (3) samarium seems to be electro-reduced into the amalgam, but back-reacts very rapidly to give samarium compounds; and (4) although only a few experiments were conducted, praseodymium seems to be electrolyzed easily, and appeared to remain in the amalgam.

The organic electrolysis experiments have not been encouraging, and no further experiments using this method of approach are planned.

C. Direct Reduction with Falling Amalgam Droplets

Barnet et al.[4] have demonstrated that rare earth amalgams can be prepared by dropping an alkali metal amalgam through a column of aqueous rare earth solution. The alkali metal exchanges directly with the rare earth ions; hence no electrolysis is involved. Therefore, a series of dropping sodium amalgam experiments was conducted using a solution of samarium-cobalt dissolved in acetic acid adjusted to pH 4. A schematic diagram of the experimental apparatus is shown in Figure 13. The samarium-cobalt ratio in the solution was varied between 1:1 and 100:1.

After reduction the mercury was vacuum distilled at 350°C, and the samples were heated briefly at 750°C to remove any traces of

---

[4] M. F. Barnet, D. S. Weasy, and N. E. Topp, J. Inorg. Nucl. Chem., 25, 1273 (1963).

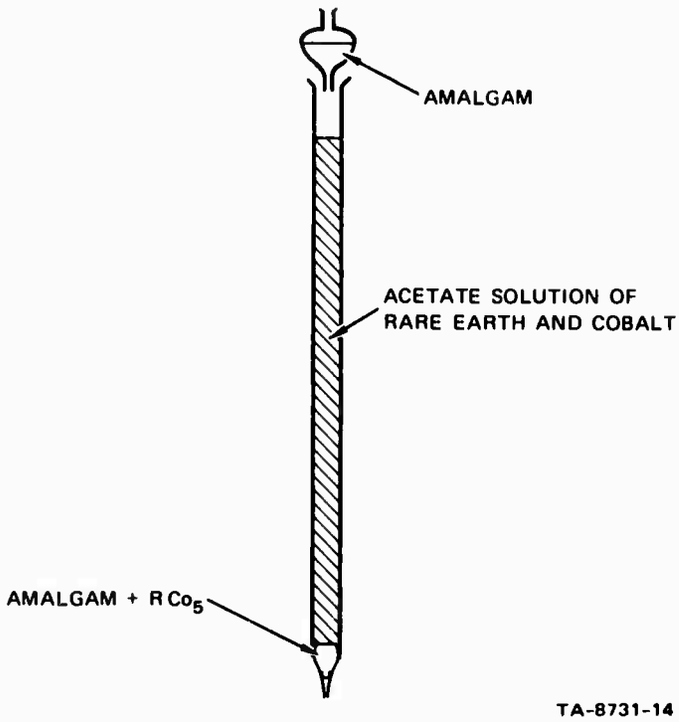

FIGURE 13 SKETCH OF A DROPPING-AMALGAM EXPERIMENT

mercury. Oxidation of the samarium-cobalt residue occurred either during the ion exchange reaction or during the mercury distillation, and therefore the residue was separated into a magnetic fraction and a nonmagnetic fraction. A summary of typical data is given in Table VIII.

Table VIII

TYPICAL RESULTS OF SODIUM AMALGAM DROPPING EXPERIMENTS

Sm/Co in Acetate Solution	Magnetic Fraction			Nonmagnetic Fraction	
	% Sm	% Co	H_{m}^{c}	% Sm	% Co
1:1	29.5	57.8	700	76.6	4.5
2:1	39.7	52.0	350	76.4	2.1
10:1	20.5	69.5	70	80.3	0.44
100:1	Nil	Nil	--	82.8	0.45

The sodium amalgam drop reduction method has yielded a powder containing samarium and cobalt. However, mutual reaction of these metals to form $SmCo_5$ or any other intermetallic compound appears to be slow at room temperature. Oxygen contamination may also contribute to low coercivities in these materials. The difficulty of obtaining samarium-cobalt powders having high coercivities is so great that research with this processing method has been terminated.

D. Precipitation from Distilling Zinc Liquid Alloy Solutions

One thermal gradient transfer experiment and six solution/precipitation experiments were conducted using a zinc-cobalt-samarium alloy melt. The results are summarized in Table IX. It was not possible to recover $SmCo_5$ after a dissolution/precipitation in a thermal gradient transfer experiment. No etchant could be found that selectively

Table IX

SUMMARY OF ZINC SOLUTION PRECIPITATION EXPERIMENTS

Run	Type of Experiment	Temp. °C	Duration	Starting Composition	Crucible	Results
DC-5	Temperature gradient transfer	600 (max.)	5 hours	$SmCo_5$ with excess zinc	Graphite	Crucible was crushed and zinc was leached; evident reaction with samarium
DC-6	Distillation/ precipitation	500	1 hour	10% $SmCo_5$ lump 90% zinc	Molybdenum	After HCl etching the residue contained only cobalt dendrites
DC-7	Distillation/ precipitation	700	4 hours	4.7% $SmCo_5$ lump 95.3% zinc	Molybdenum	The residue consisted of variable-sized particles that were 33% Sm and 67% Co, but the particles were not single crystals and may have resulted from disintegration of the $SmCo_5$ lump rather than precipitation
DC-9	Distillation/ precipitation	500	7 hours	13% $SmCo_5$ lump 87% zinc	Quartz tube	As zinc dissolved $SmCo_5$, the liquidus temperature increased and solidification of the mass occurred, little distillation of zinc
DC-10	Distillation/ precipitation	925	8 hours	5% $SmCo_5$ lump 95% zinc	Quartz tube	Only 37% of the zinc distilled
DC-14	Distillation/ precipitation	1000	Until transfer was complete	52% zinc 40% cobalt shot 8% Sm shot	Quartz tube	All of the zinc and most of the samarium were transferred; the cobalt only partially dissolved
DC-16	Distillation/ precipitation	1000	Until transfer was complete	40% $SmCo_5$ fine powder 60% zinc	Quartz tube	All of the zinc was transferred, most or all of the $SmCo_5$ dissolved and reprecipitated; particle mass was sintered into a porous core: 73% Co, 25% Sm; some residue on vessel walls: 65% Co, 26% Sm.

etches zinc without also dissolving samarium. The residue after hydrochloric acid etching was dendritic cobalt. Since a ternary phase diagram is not available, it is uncertain what phases may have precipitated.

The goal of most of the experiments was complete distillation of the zinc to avoid a subsequent acid etching treatment to remove zinc. One of the early experiments at 700°C, run DC-7, started with massive lumps of $SmCo_5$ and yielded particles with the correct $SmCo_5$ stoichiometry. These results were not reproduced in subsequent runs below 1000°C, and there is some suspicion that the lump $SmCo_5$ physically disintegrated rather than dissolving and reprecipitating as zinc was removed by distillation. The results at temperatures below 1000°C yield a zinc melt that gradually freezes as $SmCo_5$ is dissolved. Evidently Sm-Zn and Co-Zn solid phases are formed as samarium and cobalt are introduced to the zinc solution, which is consistent with the Sm-Zn and Co-Zn binary phase diagrams.

The melting points of all of the Sm-Zn and Co-Zn intermetallic compounds are below 1000°C. Distillation/precipitation experiments at this temperature result in rapid distillation and a precipitated residue that is at least approximately the composition of the starting samarium-cobalt alloy. However, the distillation is very rapid, and complete solution of the samarium and cobalt before zinc distillation and reprecipitation of a Co-Sm alloy is difficult. Since this distillation temperature exceeds the Curie temperature in situ, magnetic alignment of precipitated alloy particles is not possible. A very important problem at these temperatures occurs because the residual particles sinter. This requires grinding to produce particles for powder magnet fabrication and offers no advantage over conventional

processing. The magnetic properties of these materials are not superior to conventionally processed powders, and no further work is planned with liquid zinc alloys.

E. Direct Metallothermic Reduction

Samarium can be used to reduce a cobalt salt, and if excess samarium is used the reduced cobalt should form a cobalt-samarium alloy at elevated temperatures. Ordinarily this would melt the alloy and require subsequent grinding, but if the samarium reductant is in a fused salt solution the alloy phase may form as particles within the salt solution. In a BaF_2/LiF salt solution the stoichiometric reaction to form $SmCo_5$ would be

$$13\ Sm + 15\ CoX_2 \rightarrow 10\ SmX_3 + 3SmCo_5,$$

where X is a halide.

To test the feasibility of this approach, an isostatically pressed CoF_2 plug was inserted into a rotary crucible containing a BaF_2/LiF eutectic melt saturated with free samarium at 1050°C. After 30 minutes, rotation of the crucible was terminated and the melt was allowed to solidify. The frozen salt containing the CoF_2 plug was removed and cross-sectioned to expose the interface between the CoF_2 plug and the BaF_2/LiF melt, which is shown in Figure 14. Electron beam microprobe analyses showed that the light colored spots are cobalt particles. The CoF_2 salt matrix contained a low concentration of samarium that increased toward the interface. In the region of the interface some samarium particles were present, evidently precipitating on cooling.

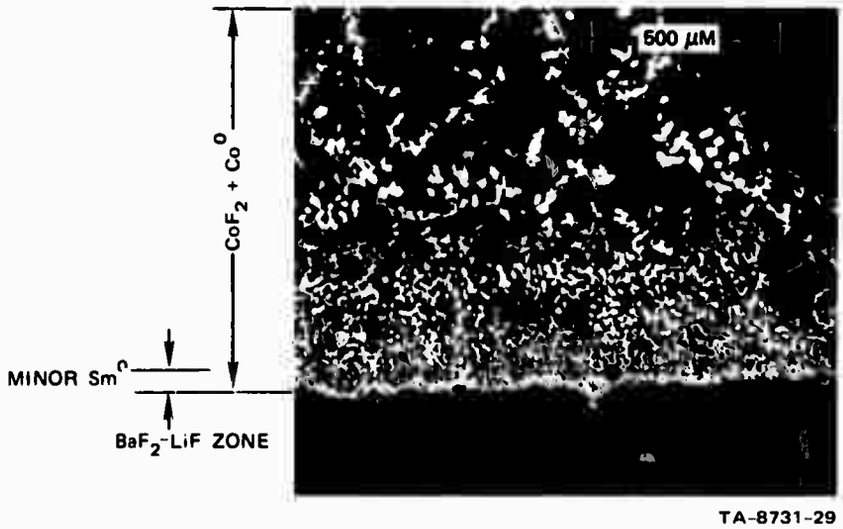

FIGURE 14 FROZEN INTERFACE BETWEEN CoF_2 AND A BaF_2-LiF FUSED SALT

Next, a thermite reduction reaction between samarium and $CoCl_2$ was conducted in vacuum and in argon using an intimate mixture of powders. Since samarium powder is difficult to grind and very reactive, a samarium-cobalt eutectic alloy that grinds easily and is less reactive was substituted. Portions of alloy and $CoCl_2$ were taken to yield a high samarium alloy and $SmCl_2$. Upon heating, this reaction occurs exothermically. The resulting alloy melted and formed spherical particles of various sizes in a salt matrix; however, many of the particles were too large for magnet powder processing. Considerable splattering also occurred. The sample was leached in a sodium acetate solution to remove the soluble salts before chemical analysis. The alloy particles contained insufficient samarium: 78% cobalt and 16% samarium. The expected alloy composition based on chemical analysis of the alloy was 75% cobalt and 25% samarium. Some of the samarium may have been lost by vaporization.

Direct reduction of $CoCl_2$ was also conducted in the presence of moderate amounts of the BaF_2/LiF eutectic as an activator to dissolve samarium and also as a heat sink to prevent a temperature excursion from the exothermic reaction and melting. The BaF_2/LiF eutectic salt was 43 wt% of the particle mixture. This mixture was heated in a tantalum crucible at 800°C for two hours without inducing a temperature excursion and then cooled. The resulting alloy particles were extremely fine and could not be physically separated from the residual salt without oxidizing the alloy particles. Consequently, a true chemical analysis of the alloy cannot be obtained. The analysis of the total residue was consistent with a materials balance on the alloy and salt phases.

Although the results from magnetic evaluation of these directly reduced alloys were poor the alloys were far from the correct $SmCo_5$ stoichiometry. Further thermometallic reduction reactions are planned to produce alloys nearer to the $SmCo_5$ composition.

F. Magnetic Evaluation of Particles Produced by Alternative Methods

Rare earth-cobalt alloy particles formed by electrolysis in fused salts, by electrolysis in organic electrolytes, by dropping amalgam experiments, or by zinc solution precipitation experiments all exhibit low coercivities and low $4\pi M_r$ values. The poor magnetic properties were caused principally by an inability to form the $RECo_5$ compound or contamination of the alloy particles with oxygen.

Results from chemical analysis, x-ray diffraction, and metallography were used to select samples for magnetic evaluation. The results are shown in Table X. Demagnetization corrections were not made in calculating the $4\pi M_r$ values.

Table X

MAGNETIC EVALUATIONS OF PARTICLES PRODUCED BY ALTERNATIVE PROCESSING METHODS

Run	Type of Experiment	H_m (Oe)	H_{mc} (Oe)	$4\pi M_r$ (G)
DC-15-1	Distillation/ precipitation	46,000	350	600
DC-16	Distillation/ precipitation	51,700	250	1078
DC-17	Fused salt electrolysis	40,000	224	--
DC-18	Direct reduction (Thermite)	51,000	1140	564
EW-11	Dropping amalgam	51,700	70	480
EW-13	Dropping amalgam	14,300	350	--
EW-14	Dropping amalgam	35,500	700	522

IV SINTERABILITY

Plasma spheroidized samarium-cobalt alloy powders were cold pressed and sintered in order to test the sinterability of these materials. A samarium-cobalt alloy was formed using 44.75 wt% samarium and 55.25 wt% cobalt. The alloy was ground in an alumina ball mill for six hours, and then the powder was spheroidized in an argon plasma. The resulting material had less samarium than the starting powder but contained two phases, Sm_2Co_7 and $SmCo_5$. The average particle composition following spheroidization is expected to be 42% samarium and 58% cobalt. The alloy powder was then pressed at 150,000 psi in a uniaxial die. During the cold-pressing operation, a magnetic field of 27,000 oersteds was applied to the sample. The sample was then sintered in a vacuum furnace at 1100°C for 30 minutes. The final fired density was 80% of the theoretical density.

Another sample of the spheroidized alloy was mixed with 18 wt% of a samarium-cobalt alloy containing 60 wt% samarium and 40 wt% cobalt and subsequently cold pressed and sintered as described above. The final fired density in the latter case was 83% of the theoretical density.

The densities achieved in these experiments compare very favorably with those reported by Cech.[5] Thus a conclusion can be made that plasma spheroidization does not decrease the sinterability of samarium-cobalt alloy powders. The spherical microstructure obtained with the sample having the higher samarium content is shown in Figure 15. The presence of a second phase is readily seen within these particles.

---

[5] R. E. Cech, J. App. Phys. 41, 5247 (1970)

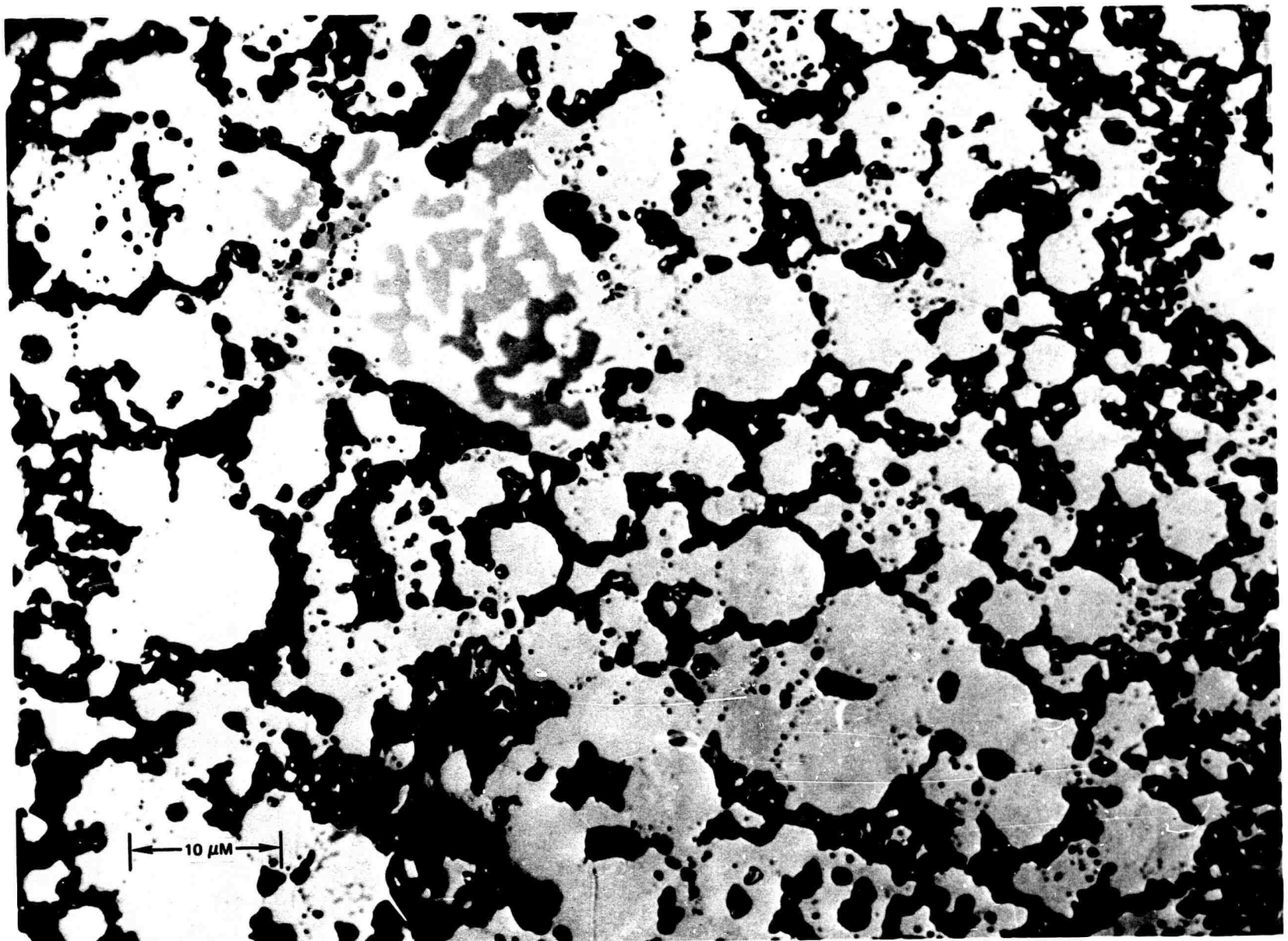

FIGURE 15 MICROSTRUCTURE OF SINTERED SPHERICAL PARTICLES OF Sm-Co ALLOY, PRIMARILY $SmCo_5$ COMPOSITION

V SUMMARY

During this research period, we have investigated the magnetic properties of rare earth-cobalt materials, produced by plasma spheroidization, plasma annealing, electrolysis in fused salts, electrolysis in organic liquids, direct reduction from amalgam droplets, precipitation from distilling zinc liquid alloy solutions and direct metallothermic reduction.

The plasma spheroidization process currently yields spherical polycrystalline particles. The remanence of these particles is consequently reduced, and due to the heating of the particles in the argon plasma, the intrinsic coercive force is also reduced. A final evaluation of the effectiveness of plasma spheroidization, must be made by sintering the spherical particles into magnets and evaluating the magnetic properties of the sintered material.

Plasma annealing results in low coercivities, but does not affect the remanence since the particles remain monocrystalline. Evaluation of the plasma annealing process should also be made after sintering of the materials.

Electrolysis in organic liquid and direct reduction from amalgam droplets yielded powder materials that did not have discernable x-ray diffraction patterns, and the coercivities of these powders were extremely low. These methods are therefore grossly inferior to comminution processes for the production of powders for rare earth-cobalt magnets.

The materials produced by precipitation from liquid zinc alloy solutions sintered during the precipitation process, and since the distillation temperature exceeded the Curie temperature, these materials required grinding prior to alignment and fabrication into permanent magnets. Thus this

method does not offer any advantage over conventional processing techniques.

Electrolysis from fused salts and direct metallographic reduction have not been fully explored and further research is required before an evaluation of these processes can be made.

VI FUTURE WORK

Plasma spheroidization and plasma annealing studies of $SmCo_5$ and $PrCo_5$ will be continued, and the processing steps will be evaluated by measuring the intrinsic coercive force and remnance before and after sintering of the materials into magnets.

A study will be made of the sintering process to achieve lower sintering temperatures and a less sensitive procedure. This study will encompass such variables as solubility, composition of the liquid phase, distribution of the liquid phase, grain size, time and temperature, and a correlation of these variables with magnetic properties.

A brief investigation of the effect of oxygen on the magnetic properties of rare earth-cobalt alloys will be conducted by studying the oxidation kinetics at low oxygen and low water vapor pressures. In addition to the oxidation study, an attempt will be made to determine the oxygen solubility and oxygen diffusivity in rare earth-cobalt alloys.

Appendix I

DETERMINATION OF RARE EARTH AND COBALT IN RARE EARTH-COBALT ALLOYS

This determination includes both elements and is based on the chelometric titration of the total rare earth and cobalt content with ethylene-diaminetetra-acetic acid (EDTA) and the subsequent titration of the liberated EDTA after masking the rare earth content with fluoride. The fundamental reactions are

$$Co + EDTA \longrightarrow Co\text{-}EDTA$$

$$RE + EDTA \longrightarrow RE\text{-}EDTA$$

and

$$RE\text{-}EDTA + F^{-} \xrightarrow{pH\text{-}5} RE\text{-}F + EDTA$$

$$EDTA + Zn \xrightarrow{pH5} Zn\cdot EDTA\ .$$

Reagents

Acetate buffer, pH 5: Dissolve 160 g of reagent grade anhydrous sodium acetate or 270 g of the trihydrate in 500 ml water. Add 60 ml of glacial acetic acid and dilute to a liter.

Xylenol orange indicator: Dissolve 0.1 g of the indicator in 100 ml of deionized water (Stable).

0.1000 M EDTA: Dissolve 37.23 g of the disodium salt in 800 ml of deionized water in a plastic beaker and dilute to a liter. If the purity of the EDTA is not known, standardize against the zinc standard solution.

0.02000 M zinc solution: Dissolve 1.3076 g of the pure metal in a minimum amount of hydrochloric acid and dilute to a liter.

Procedure

Approximately 100 to 125 mg of the alloy is weighed into a 400-ml beaker. The alloy is covered with a small quantity of water plus 2 ml of hydrochloric acid and placed on a hot plate (low temperature) to dissolve the alloy. (Nitric acid is added if any resistance particles remain.) The solution is evaporated to dryness, and 4 ml of the buffer is added to dissolve the salt.

Approximately 300 ml of hot water plus 1/2 ml of pyridine are added, and immediately before titration with EDTA, a few crystals of ascorbic acid and five or six drops of the indicator are added. The solution is titrated to a color change from purple to yellow-orange (Titration 1). Then, approximately 0.3 of solid ammonium bifluoride plus 0.5 g of solid boric acid are introduced and dissolved. The amount of EDTA liberated is titrated with zinc solution (Titration 2). A blank should be run on all reagents. A comparison of EDTA and zinc titrants is made in the same titration beaker that contained all the contents of the determination.

Calculations

% Co
= {[ml EDTA Titration 1 - m/EDTA equiv. to m/Zn solution Titration 2]
x [molarity EDTA x 58.933 mg/m mole x 100]} /wt of sample in mg

% RE
= {[m/EDTA Titration 2] x [molarity EDTA x atomic wt of RE x 100]} /wt of sample in mg

Appendix II

PROCEDURE FOR PRODUCING MAGNETOMETER SPECIMENS OF POWDERS

Magnetometer samples are prepared by mixing the rare earth-cobalt alloy powders with a fast-setting epoxy binder. The mixture is then placed in a magnetic field for alignment while the epoxy hardens. The binder consists of eight parts by weight of Epon 826, two parts of Epon 812, and one part of Triethylenetetraamine. This mixture is placed in a vacuum dissicator for outgassing. A known quantity of rare earth-cobalt powder is then mixed with the epoxy mixture and outgassed. Polyethylene tubes 1/8 inch inside diameter and 1/4 inch long are then filled with the mixture of epoxy and $RECo_5$.

The ends of the polyethylene tubes are sealed with plastic tape and placed into a sample holder within the air gap of a Varian V4004 4-inch magnet. The samples are subjected to magnetic fields of 14,000 oersteds and the temperature is raised to $40^{o}C$. The magnetic field and temperature are held constant for 16 hours to ensure setting of the epoxy. The epoxy-rare earth-cobalt samples are then extruded from the polyethylene tubes and are ready for measurement in the P.A.R. vibrating magnetometer.